tion

Impaired motor axon regeneration in the
urol., **333**, 449–454.
rstrand, G. (1965) Proprioceptive innervation
ond.), **178**, 161–171.
ronal determinants of regeneration. *Trends*

1972) Nerve conduction during Wallerian
urol. Neurosurg. Psychiatr., **35**, 335–341.
i. (1978) Role of the cell body in axonal
ed.), *Neuronal Plasticity*. Raven Press, New

Long-term increase in the levels of c-*jun*
unoreactivity in motor and sensory neurons
i. Lett., **129**, 107–110.
P. and Gordon, S. (1991) Heterogeneity in
f microglia in the normal adult mouse brain.

avo, R. (1991) Selective expression of Jun
axonal transport block in peripheral nerves
the regeneration process. *Brain Res.*, **566**,

Klebanoff, S. J. (1983) Increased respiratory
it monocytes. *Blood*, **62**, 902–909.
, M. C., Rosen, H. and Gordon, S. (1989)
n does not hinder regeneration in peripheral nerve. *Eur. J. Neurosci.*, **1**, 27–33.

Lyon, M. F., Ogunkalade, B. W., Brown, M. C., Atherton, D. J. and Perry, V. H. (1993) A gene affecting Wallerian degeneration maps distally on mouse chromosome 4. *Proc. Natl. Acad. Sci. USA*, **90**, 9717–9720.

McCormack, M. L., Goddard, M., Guenard, V. and Aebischer, P. (1991) Comparison of dorsal and ventral root regeneration through semipermeable guidance channels. *J. Comp. Neurol.*, **313**, 449–456.

McQuarrie, I. G. and Grafstein, B. (1973) Axon outgrowth enhanced by a previous nerve injury. *Arch. Neurol.*, **29**, 53–55.

Mirsky, R., Jessen, K. R., Schachner, M. and Goridis, C. (1986) Distribution of the adhesion molecules NCAM and L1 on peripheral neurons and glia in the adult rat. *J. Neurocytol.*, **15**, 795–815.

Perry, V. H. and Brown, M. C. (1992) Role of macrophages in peripheral nerve degeneration and repair. *BioEssays*, **14**, 401–406.

Perry, V. H., Brown, M. C. and Gordon, S. (1987) The macrophage response to central and peripheral nerve injury. A possible role for macrophages in regeneration. *J. Exp. Med.*, **165**, 1218–1223.

Perry, V. H., Brown, M. C. and Lunn, E. R. (1991). Very slow retrograde and Wallerian degeneration in the CNS of C57BL/Ola mice. *Eur. J. Neurosci.*, **3**, 102–105.

Perry, V. H., Brown, M. C. and Tsao, J. W. (1992) The effectiveness of the gene which slows Wallerian degeneration in C57BL/Ola mice declines with age. *Eur. J. Neurosci.*, **4**, 1000–1002.

Sjoberg, J. and Kanje, M. (1990) The initial period of peripheral nerve regeneration and the importance of the local environment for the conditioning lesion effect. *Brain Res.*, **529**, 79–84.

European Journal of Neuroscience, Vol. 6, pp. 429–453

Differential Foci and Synaptic Organization of the Principal and Spinal Trigeminal Projections to the Thalamus in the Rat

Matthew N. Williams, Daniel S. Zahm and Mark F. Jacquin
Department of Anatomy and Neurobiology, St. Louis University School of Medicine, 1402 South Grand Boulevard, St Louis, MO 63104, USA

Key words: barrel, vibrissa, somatosensory, convergence, divergence, fluorescent dextrans, parvalbumin, calbindin, electron microscopy

Abstract

The thalamus is known to receive single-whisker 'lemniscal' inputs from the trigeminal nucleus principalis (PrV) and multiwhisker 'paralemniscal' inputs from the spinal trigeminal nucleus (SpV), yet the responses of cells in the thalamic ventroposteromedial nucleus (VPM) are most similar to and contingent upon inputs from PrV. This may reflect a differential termination pattern, density and/or synaptic organization of PrV and SpV projections. This hypothesis was tested in adult rats using anterograde double-labelling with fluorescent dextrans, horseradish peroxidase (HRP) and choleragenoid, referenced against parvalbumin and calbindin immunoreactivity. The results indicated that PrV's most robust thalamic projection is to the whisker-related barreloids of VPM. The SpV had robust projections to non-barreloid thalamic regions, including the VPM 'shell' encapsulating the barreloid area, a caudal and ventral region of VPM that lacks barreloids and PrV inputs, the posterior thalamic nucleus, nucleus submedius and zona incerta. Within the barreloid portion of VPM, SpV projections were sparse relative to those from PrV, and most terminal labelling occurred in the peripheral fringes of whisker-related patches and in inter-barreloid septae. Thus, PrV and SpV have largely complementary projection foci in the thalamus. Intra-axonal staining of a small sample of trigeminothalamic axons with whisker or guard hair receptive fields revealed highly localized and somatotopic terminal aggregates in VPM that spanned areas no larger than that of a single barreloid. In the electron microscopic component of this study, HRP transport to the barreloid region of VPM from left SpV and right PrV in the same cases revealed PrV terminals contacting dendrites with a broad range of minor axis diameters (mean ± SD: 1.51 ± 0.10 μm). SpV terminals were indistinguishable from those of PrV, but they had a disproportionate number of contacts on narrow dendrites (1.27 ± 0.07 μm, $P < 0.01$). PrV endings were also more likely to contact VPM somata (11.0 ± 4.2% of all labelled terminals) than those from SpV (3.0 ± 1.0%, $P < 0.01$). Insofar as primary dendrites are thicker than distal dendrites in VPM, these data suggest a differential distribution of PrV and SpV inputs onto VPM cells that may account for their relative efficacies in dictating the responses of VPM cells to whisker stimulation. Multiwhisker receptive fields in VPM may also reflect direct transmission of convergent inputs from PrV.

Introduction

The rodent trigeminal (V) system, in particular those portions devoted to processing inputs from the mystacial whiskers, is a widely used model system for studying mechanisms underlying neuronal information processing, pattern formation and plasticity (see White, 1989; Woolsey, 1990; Killackey *et al.*, 1990; Jones and Diamond, 1994, for the most recent reviews). Although general features of the subcortical whisker pathways are now well delineated, various important aspects of subcortical V circuitry remain unknown. This is especially true for the thalamic nuclei, including the ventroposteromedial nucleus (VPM).

In rodents, VPM is known to receive substantive inputs from the V nucleus principalis (PrV), each of spinal V subnuclei oralis (SpVo), interpolaris (SpVi) and caudalis (SpVc), infragranular layers of the cortical barrelfield, and the thalamic reticular nucleus (e.g. Jones, 1985; Ohara and Lieberman, 1985; Jacquin *et al.*, 1986a; Bruce *et al.*, 1987; Hoogland *et al.*, 1987, 1988; DeBiasi *et al.*, 1988; Welker *et al.*, 1988; Killackey *et al.*, 1989; Chmielowska *et al.*, 1989; Chiaia *et al.*, 1991a, b; Lee *et al.*, 1993), and to lack interneurons (Barbaresi *et al.*, 1986) and recurrent axon collaterals (Harris, 1986, 1987; Chiaia *et al.*, 1991b). However, certain aspects of VPM circuitry require resolution in order to gain a more complete understanding of the anatomical bases for the response properties of VPM cells. For example, it remains unclear why inputs from thalamic-projecting SpV cells ('paralemniscal'), whose receptive fields include multiple whiskers (Woolston *et al.*, 1982; Renehan *et al.*, 1986; Jacquin *et al.*, 1986a, 1989; Jacquin and Rhoades,

1990), are not expressed in the vast majority of VPM cells, whose receptive fields include one whisker (Waite, 1973; Brown and Waite, 1974; Rhoades *et al.*, 1987; Ito, 1988; Sugitani *et al.*, 1988; Lee *et al.*, 1993), whereas 'lemniscal' inputs from PrV single-whisker cells are (Jacquin *et al.*, 1988). To account for their observation that convergent inputs from SpV are only expressed in VPM cells after PrV ablations, Rhoades *et al.* (1987) hypothesized that VPM receptive fields may more faithfully express PrV receptive fields because of a differential termination pattern and density of PrV and SpVi inputs on VPM dendrites.

The results of five recent studies suggest that under appropriate anaesthetic and recording conditions most VPM cells do express multiwhisker inputs. Simons and Carvell (1989), Armstrong-James and Callahan (1991), Diamond *et al.* (1992a) and Friedberg *et al.* (1993a, b) reported multiwhisker receptive fields in rats lightly anaesthetized with fentanyl or urethane, and Chiaia *et al.* (1991b) described excitatory postsynaptic potentials induced by stimulation of SpV or neighbouring whiskers in VPM cells with single-whisker receptive fields. As noted by Chiaia *et al.* (1991b), there is no obvious reason why inputs from SpV should be differentially affected by anaesthesia, in the light of the available data suggesting similarities in the anatomical features of synapses in VPM made by axons from different portions of the V brainstem complex (Peschanski *et al.*, 1985). These data, however, are consistent with the notion that PrV and SpV inputs to VPM have overlapping distributions, as has been shown for the analogous spinal and dorsal column pathways (Ma *et al.*, 1986, 1987).

Further anatomical studies are therefore required to assess the organization of PrV 'lemniscal' and SpV 'paralemniscal' inputs to VPM, and the thalamus in general. The present study addresses this issue by determining the extent to which PrV and SpV inputs to thalamus are complementary or overlapping, using a number of anterograde labelling paradigms and light and electron microscopic analyses.

Parts of this work have been reported in abstract form (Williams *et al.*, 1993).

Materials and methods

Adult Sprague–Dawley rats of both sexes were used. Housing and treatment conditions adhered to institutional and federal guidelines. Rats were anaesthetized during all surgical procedures as follows: experiment 1, ketamine 45 mg/kg i.p. and xylazine 7 mg/kg i.p.; experiments 2 and 3, sodium pentobarbitone 65 mg/kg i.p. and atropine sulphate 0.05 mg/kg i.p. Supplementary doses were given during lengthy operations. The scalp and neck musculature were also injected with 2% lidocaine HCl and adrenaline (1:50 000 ISU). All animals were mounted in a stereotaxic frame and kept warm with a heating pad. Tracer injections in experiments 1 and 3 were made under stereotaxic guidance through glass micropipettes with a tip inside diameter of ~50 μm and made using a hydraulic microdrive-driven ejection apparatus. After varying survival intervals, rats were deeply anaesthetized with sodium pentobarbitone prior to being killed by intracardiac perfusion.

Experiment 1: light microscopy, bulk labelling

To assess the projections in the right thalamus from PrV and SpV, injections of fluorescent dextran were made into the left SpVi, and either cholera toxin subunit B (CTB) or wheatgerm agglutinin–horseradish peroxidase (WGA–HRP) was injected into the left PrV. Seventy animals were used for experiment 1.

Tracer injections

Seven to 14 days prior to killing the rats, either fluorescein dextran or rhodamine dextran (10% in distilled water; Molecular Probes, products D-1820 and D-1817 respectively) was injected in SpVi. The cisterna magna was opened to expose the surface of the brainstem. Pressure injections (8–16×200 nl deposits along each track) were made in SpVi using an angled approach, 45° from the vertical, medial 25° from the anteroposterior axis. The caudalmost tracks were placed level with the obex and the rostralmost tracks 2.0 mm anterior to this point. Two days before the animals were killed, they received injections of CTB tagged with fluorescein (1% in distilled water; List product 106) into the right PrV. Five closely spaced injection tracks (a total of 200 nl of tracer in each track) were made at the following coordinates: posterior to lambda 0.3, 0.6, 0.9, 1.2, 1.6 mm, and laterally alternating between 2.7 and 3.0 mm to the midline. In the remaining animals, 12 h before processing, PrV received similarly placed injections (120 nl per track) of WGA–HRP (5% in 0.1 M Tris buffer, pH 8.6; Sigma).

Fixation and histochemistry

Perfusion was initiated with saline followed by 500 ml of 4% paraformaldehyde in 0.1 M sodium phosphate buffer, pH 7.4. The brains were removed, cryoprotected overnight in 30% sucrose buffer, and cut in two transversely through the midbrain before sectioning on a freezing microtome at 40 μm. Sections were harvested in four serially adjacent series. Blocks containing the diencephalon were sectioned horizontally, and the brainstems were cut coronally, to best reveal whisker-related somatotopy and subnuclear borders. One series of sections from the thalamus and one from the pons/medulla were prepared for fluorescence microscopy by mounting on subbed slides, air-drying overnight, dehydrating rapidly and clearing in xylene prior to coverslipping in Fluoromount.

Other sections were stained using antibodies to enhance and stabilize the fluorescent dextran labelling and in other sections to stain for CTB. At room temperature with gentle agitation, sections were first washed in Tris-buffered saline (0.05 M Tris, pH 7.6, 0.85% NaCl) with 0.4% Triton X-100 (TBS–TX) and then processed to reveal one of the labels. The sections were incubated overnight in 2% normal serum (goat for the fluorescent labels and rabbit for CTB) with 0.05% sodium azide and incubated in primary antisera (in TBS–TX with 0.05% sodium azide) for 15–24 h. The antisera used were biotinylated rabbit anti-fluorescein (1:250; Molecular Probes; product A-982), a rabbit anti-rhodamine (diluted 1:2500; gift of Dr Howard Chang), and a goat anti-cholera toxin B (1:20 000; List product 703). The sections were then washed in TBS–TX (3×10 min) and reincubated in an appropriate biotinylated secondary antibody (1:200; goat anti-rabbit for the fluorescent labels and rabbit anti-goat for CTB; Vector Labs) in TBS–TX with 2% normal serum for 2 h. The sections were rinsed again for 30 min and incubated in avidin–biotin–peroxidase complex (ABC; 1:200; Vector Labs) in TBS–TX for 1–2 h. After a wash in 0.1 M sodium phosphate buffer (pH 7.6, 30 min), the sections were reacted for peroxidase activity in 0.05% diaminobenzidine, 0.08% nickel ammonium sulphate and 0.005% hydrogen peroxide in 0.1 M sodium phosphate buffer for 6–8 min to produce a black reaction product.

In other sections, to reveal one of the fluorescent dextrans and CTB in the same tissue, sections were treated with 2% normal horse serum in TBS–TX with 0.05% sodium azide overnight and incubated in a medium containing a mixture of two primary antibodies, one against either fluorescein or rhodamine and the other against CTB (same antibodies and dilutions as above). These sections were then processed as above to stain for the fluorescent labels and reacted to produce a black reaction product with diaminobenzidine and nickel. Next, to reveal the CTB, the sections were washed for at least 1 h in TBS–TX with 2% normal horse serum, treated with biotinylated secondary antibody (1:200; horse anti-goat, Vector Labs) and ABC as described above. The sections were then reacted for peroxidase with diaminobenzidine to produce a brown reaction product.

To precisely delineate PrV and SpV projections relative to thalamic nuclear boundaries, tissues were processed for parvalbumin or calbindin immunoreactivity. These procedures were essentially the same as those described above, except the antisera were a mouse anti-parvalbumin

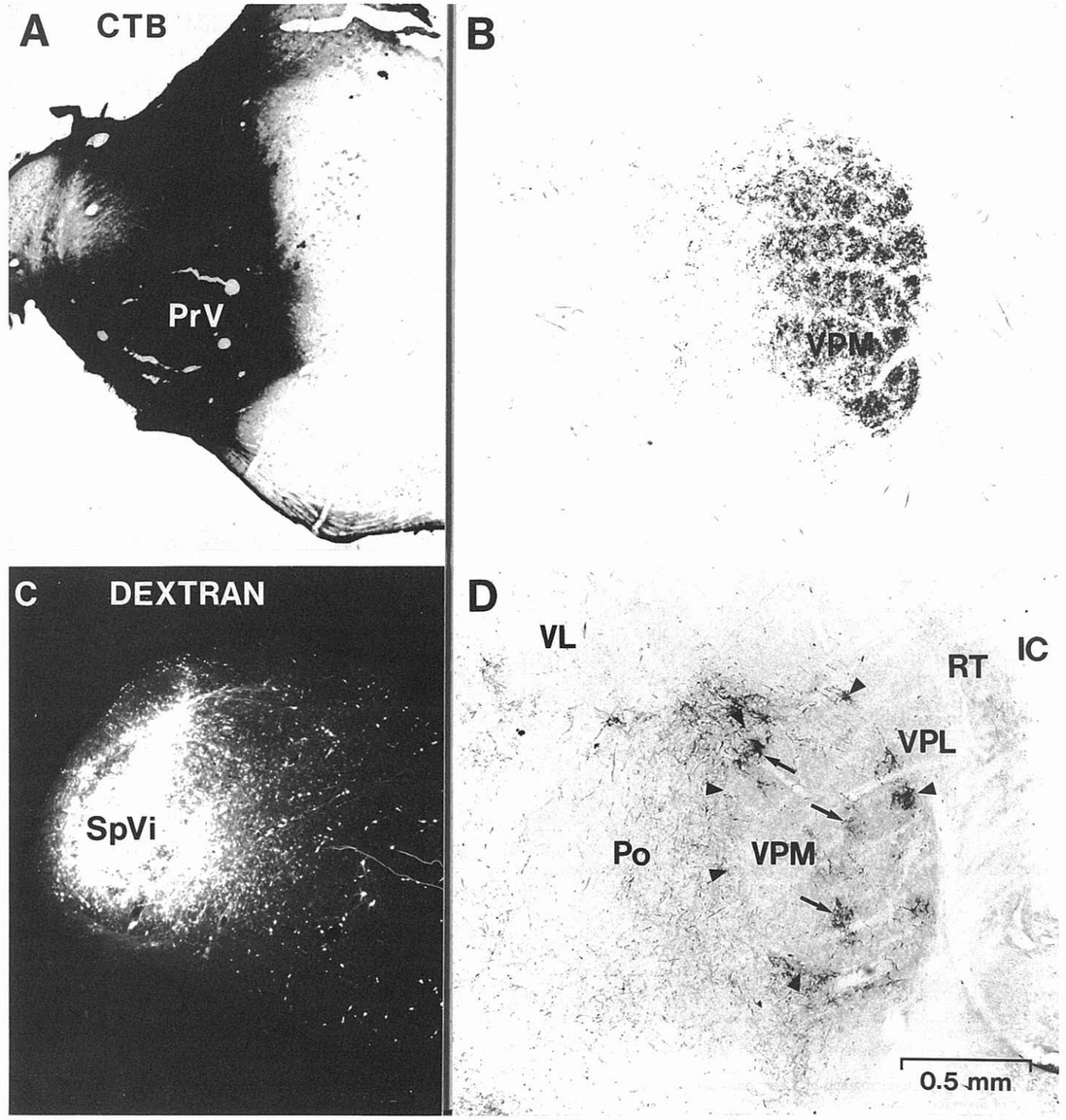

FIG. 1. Bright-field (A, B, D) and epifluorescence (C) photomicrographs of a choleratoxin B-fluorescein (CTB, 1.0 μl total volume) injection in the left nucleus principalis (PrV) and a rhodamine dextran (1.2 μl total volume) deposit in the left subnucleus interpolaris (SpVi) 2 and 12 days before the animals were killed, respectively. The PrV injection site also included the parabrachial region and the brainstem reticular formation; the SpVi injection site also included reticular formation and rostral subnucleus caudalis. This double-labelling paradigm permitted within-animal comparisons of the projection patterns of PrV and SpVi in the right thalamus (B and D, respectively). Fluorescent labelling shown in A, B and D has been immunohistochemically stabilized. Note the whisker-related patterning of the PrV projection, and the absence of such patterns in the SpVi projection. The latter is patchy in VPM (arrows); the VPM 'shell' is indicated by arrowheads. A and C are transverse sections (dorsal is up, lateral is left); B and D are horizontal sections (rostral is up, lateral is right). IC, internal capsule; Po, posterior nucleus; RT, reticular nucleus; VL, ventrolateral nucleus; VPL, ventroposterolateral nucleus; VPM, ventroposteromedial nucleus.

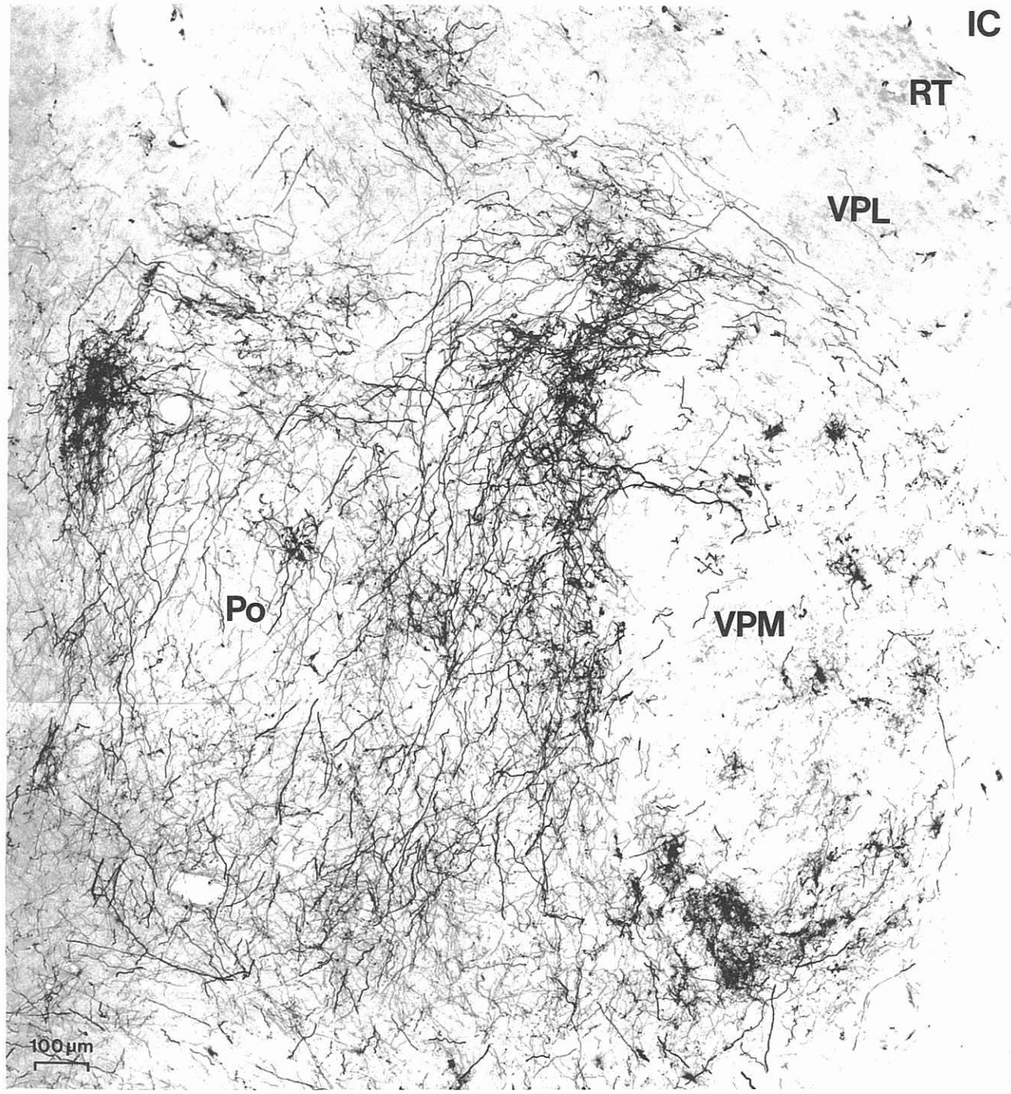

FIG. 2. Bright-field photomicrograph of a horizontal section through the right and dorsal VPM and PO showing the SpV projection, as revealed by anterograde transport of fluorescein dextran. The label was enhanced immunochemically with an antibody to fluorescein and the ABC peroxidase method. SpV fibres terminate heavily in PO and the VPM 'shell', and less significantly in VPM. Labelling in VPM is shown at higher magnification in Figures 6–8. Rostral is up; medial is left.

(1:5000; Sigma) and a rabbit anti-calbindin (1:3000; gift of Dr Ken Bainbridge). For both antibody procedures, 2% normal goat serum was used to block non-specific staining and the biotinylated second antibodies used were a rabbit anti-mouse (1:200; Sigma) and a goat anti-rabbit (1:200; Vector Labs), respectively. The sections were reacted using the nickel diaminobenzidine procedure described above for 2–4 min.

Sections for fluorescence microscopy were mounted in Fluoromount, and all other sections were mounted in DPX (Gurr) and viewed under bright-field and fluorescence optics on a Nikon Optiphot microscope. Particular attention was paid to the relative densities, locations and patterns of PrV and SpV projections.

In five other rats not receiving tracer injections, additional procedures were used to confirm the locations of thalamic nuclear borders. Four alternating series were stained for acetylcholinesterase activity, Nissl substance (cresyl violet), myelin (luxol fast blue), or both Nissl and myelin, using conventional methods.

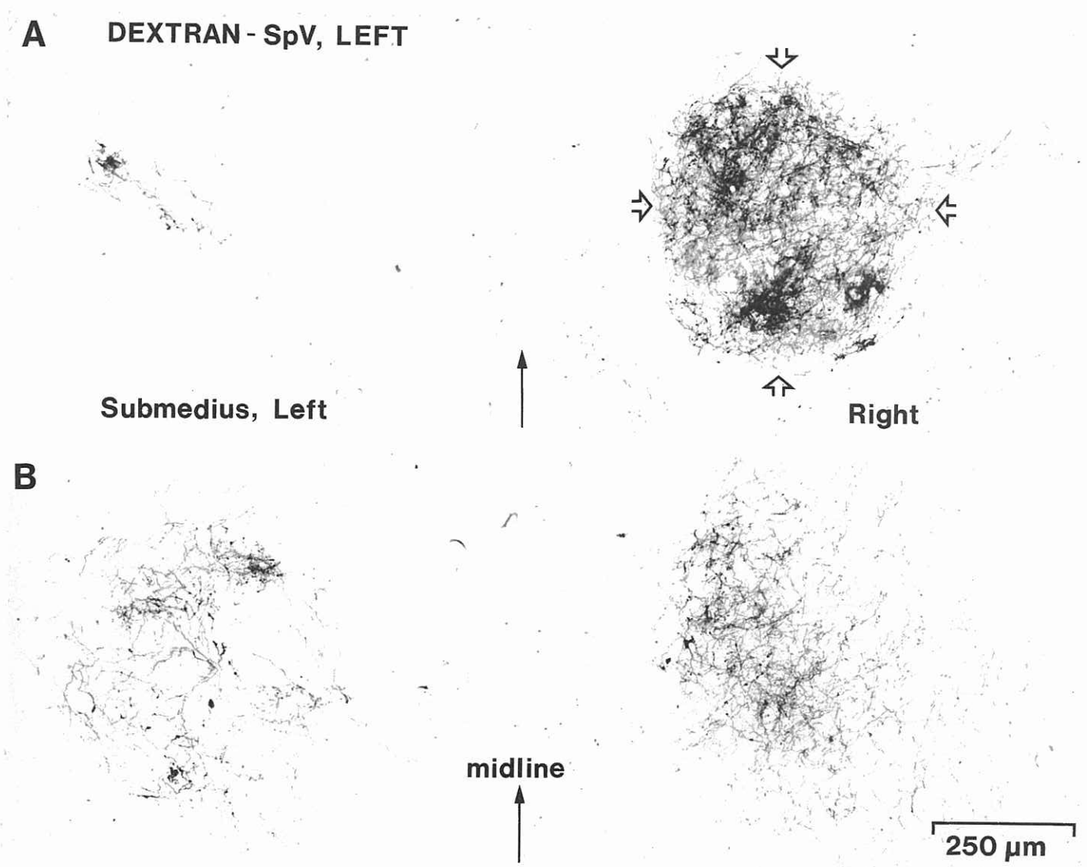

FIG. 3. Midline thalamic regions in two horizontal sections through the dorsal half of nucleus submedius showing rhodamine dextran-labelled projections from the left SpV. A is 160 µm dorsal to B. Open arrows delimit the boundaries of the nucleus submedius contralateral to the injection site and the heaviest terminal labelling. The midline is indicated by solid arrows. The strongest ipsilateral projection is shown in B and it occurs ventral to the site of the heaviest contralateral inputs (A).

Experiment 2: light microscopy, intra-axonal labelling

Insofar as nothing is known regarding the terminal morphologies of physiologically characterized V-thalamic axons, and such information would be useful in interpreting the results of experiments 1 and 3, six adult rats were prepared for intra-axonal recording and HRP injection using published protocols (Jacquin *et al.*, 1986a–c). Briefly, animals were anaesthetized, tracheotomized, secured in a headholder, immobilized with gallamine triethiodide, artificially respirated and warmed. HRP-filled, bevelled microelectrodes were directed at the medial portion of the medial lemniscus in the diencephalon after removing the overlying cortex by aspiration. Single axons were recorded with a Eutectics 400B preamplifier, receptive fields mapped, and response properties tested with a variety of hand-held probes. The axon's origin was determined by bipolar electrical stimulation of the contralateral PrV and SpVi. The V subnucleus that when electrically stimulated produced the shortest latency, high-frequency, one-to-one activation of the recorded axon was considered the axon's source. After impaling the axon, HRP was ejected by passing 2–10 nA, 250 ms positive pulses at 2 Hz for 1–10 min. No more than two fibres were injected in each case. Rats were perfused and transverse frozen sections of the diencephalon were collected at 100 µm. Sections were reacted by cobalt-intensified diaminobenzidine histochemistry. All portions of the recovered axons were reconstructed with a 40× objective and a drawing tube.

Experiment 3: electron microscopy, bulk labelling

To compare the ultrastructure and synaptic organization of PrV and SpV projections in VPM, in the same animal, HRP injections were made into PrV and SpVi on opposite sides of the brain in 18 animals.

Tracer injections

HRP (30%, Sigma type VI in 1% dimethyl sulphoxide) was injected into the left SpVi (two to five tracks, 80–200 nl per track) and right PrV (200 nl at four depths indicated below) using above-described methods, the exception being that only four deposits were made in PrV, one at each of 7.5, 7.0, 6.5 and 6.0 mm ventral to the pial surface at 0.9 mm posterior to lambda and 2.8 mm from the midline.

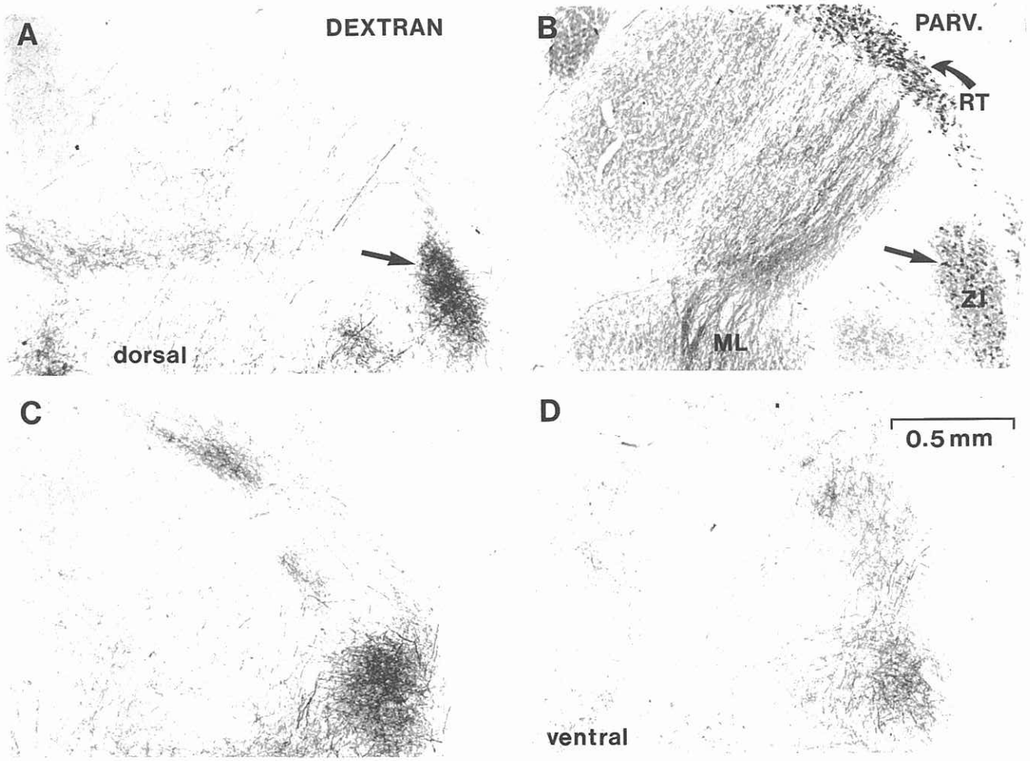

FIG. 4. Rhodamine dextran-labelled, left SpV projections (A, C, D) to, and parvalbumin (PARV.) immunoreactivity (B) in, right thalamic regions at the level of, and ventral to, the medial lemniscus (ML) in a series of horizontal sections. The section shown in B intervenes between A and C. Dextran- and parvalbumin-labelled fibres can be seen in the ML. Dense terminal labelling can be seen in the zona incerta (ZI), notably in its lateral and caudal aspects (arrows at corresponding points in A and B). Note that parvalbumin staining clearly delineates the ZI. The sections showing dextran labelling are spaced at 160 μm intervals. Rostral is up; medial is left.

Fixation and histochemistry

Two days after injection of HRP, animals were reanaesthetized and perfused with a balanced salt solution for 1 min, followed by 1 l of 2.5% glutaraldehyde in 0.1 M sodium phosphate buffer (pH 7.4 with 0.02 mM calcium chloride) for 1 h, followed by 1 l of 0.1 M sodium phosphate buffer (pH 7.4 with 0.02 mM calcium chloride). The brains were cut transversely through the midbrain for processing to enable both light microscopic assessment of the tracer injection sites and electron microscopic assessment of anterograde labelling in VPM. Brainstem blocks containing the injection sites were cryoprotected for several hours in 10% buffered sucrose, sectioned coronally on a freezing microtome at 50 μm and processed for diaminobenzidine histochemistry with cobalt chloride intensification (Adams, 1981). Injections were evaluated with bright-field and dark-field optics. Blocks containing the diencephalon were sectioned in the horizontal plane at 50 μm on an Oxford Vibratome and the sections divided into two series. All sections were processed for tetramethylbenzidine (TMB) HRP cytochemistry as follows. The first series was prepared for light microscopy according to Mesulam (1982) and the second was processed for combined light and electron microscopic analyses using Schonitzer and Hollander's (1981) procedure. For the latter, the sections were collected in 0.1 M citric acid ammonium acetate buffer, pH 6.0; preincubated in TMB medium (0.05% TMB, 2.5% ethanol, 0.15% sodium nitroferricyanide, in 0.1 M citric acid–ammonium acetate buffer, pH 6.0) for 10 min and reacted for 8 min by the addition of 0.005% hydrogen peroxide. The sections were rinsed in the above buffer and the reaction product stabilized over 15 min with cobalt chloride and diaminobenzidine (Rye *et al.*, 1984).

Processing for electron microscopy

Sections through the thalamus containing HRP-labelled fibres and terminals were postfixed in 1% osmium tetroxide for 1 h, dehydrated in ethanol and embedded in Eponate resin (Pelco). All sections were mounted between silicone-coated microscope slides and coverslips (Aldes and Boone, 1984), and the resin cured at 60°C for 36 h. Selected sections were viewed and photographed in the light microscope. After removal of the slides and coverslips, selected and matching portions of the left and right barreloid region of VPM were removed, re-embedded and serially thick- and thin-sectioned for further detailed light and electron microscopic analyses. For electron microscopy, thin sections were cut on an ultramicrotome (Ultracut E) and picked up on formvar-coated

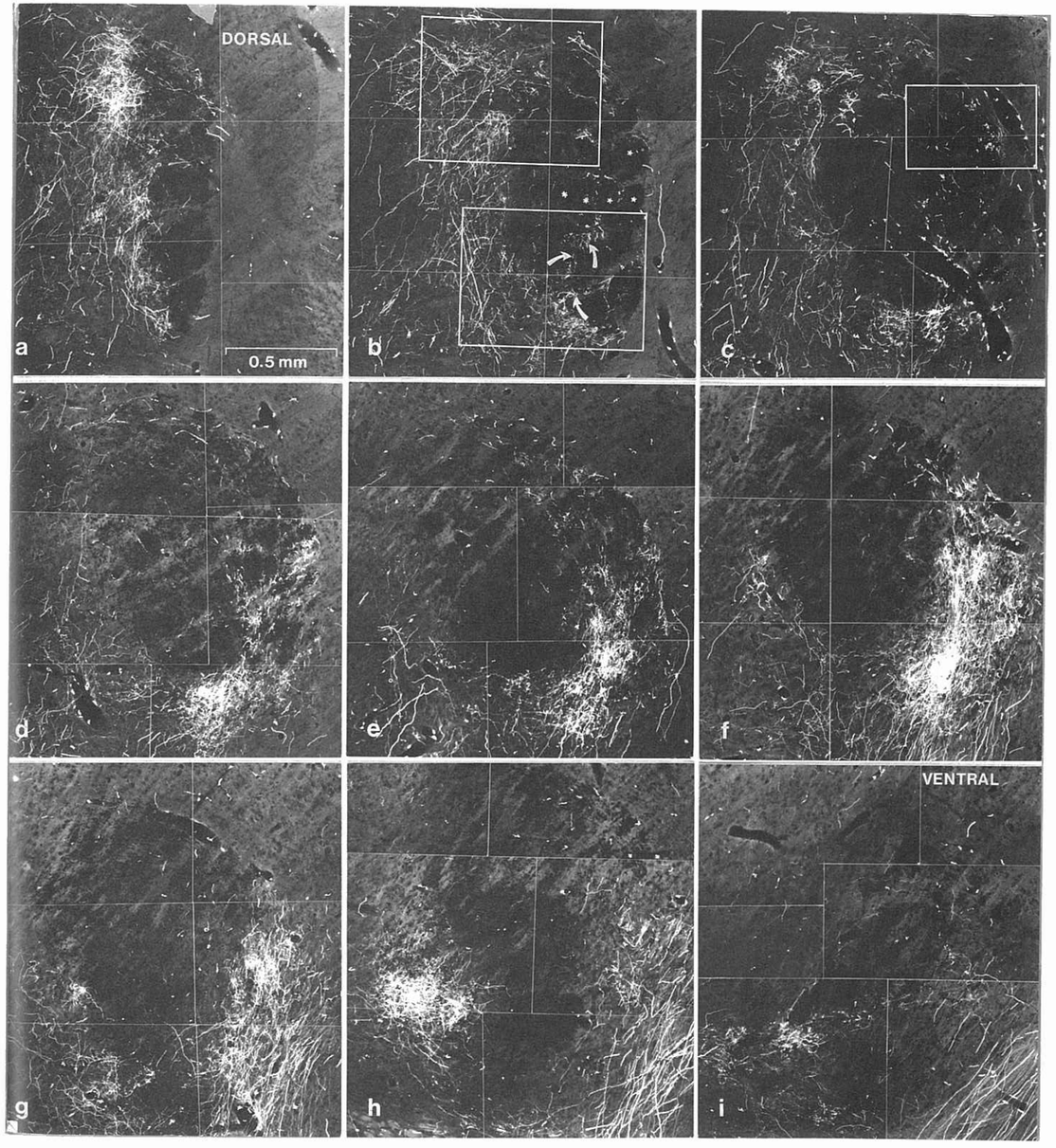

FIG. 5. SpV (white) and PrV (black) projections in montages of a series of 40 μm horizontal sections spaced at 160 μm intervals spanning the dorsal (a) to ventral (i) extent of VPM. See Figure 1 for injection sites. The rhodamine dextran-labelled SpV inputs are shown with epifluorescence optics; the CTB-labelled PrV inputs are shown with low-intensity bright-field optics. Note the complementary distributions of SpV and PrV fibres. The patchy PrV projection is concentrated within and defines the VPM barreloids; b is also shown in Figure 1B; asterisks in b identify four individual barreloids representing one row of whiskers. SpV projections are most pronounced in PO (medial to barreloids), the VPM shell encapsulating the barreloids, posteroventrolateral VPM (e–h), and interbarreloid septae and barreloid fringes (curved arrows in b). The boxed regions in b are shown at higher magnification in Figure 6; the boxed region in c is illustrated further in Figure 7. In each plate rostral is up; medial is left.

single-slot or parallel-bar grids, stained with uranyl acetate and lead citrate, and examined in a Zeiss 109 electron microscope at 70 kV.

Data analysis

Seven cases provided injection sites spanning most of PrV and SpV, and dense anterograde labelling in the left and right VPM that was readily discernible in the electron microscope. In these cases, the minor axis diameter of the postsynaptic dendrites of anterogradely labelled PrV (in left VPM) and SpV (in right VPM) synaptic boutons, and the frequency of their synaptic contact with neuronal cell bodies, were assessed from either electron micrographs or directly from the electron microscope using an attached camera lucida drawing apparatus and a digitizing tablet interfaced with a Eutectics serial reconstruction system. Thin sections were systematically scanned in such a way that no part of the section was viewed more than once and postsynaptic structures associated with every labelled bouton were included in the sample if they clearly formed a synaptic contact, as judged by the presence of a membrane specialization and associated concentrations of synaptic vesicles.

Results

Experiment 1

The following observations were made in 12 cases where tracer injections filled most of PrV, with no spread into SpV, and revealed a complete whisker-related projection pattern in VPM. These stipulations were reliably met in animals where CTB was injected into PrV. Figure 1 shows the maximal extent of an injection site and the resultant anterograde labelling in the dorsal thalamus. PrV fibres terminated most heavily within the whisker-related barreloid areas of VPM and less heavily in the posterior nucleus (PO) and zona incerta. PrV's patchy projection to VPM was somatotopically patterned and single-whisker representations were readily discerned, thus defining the VPM barreloid region. In the section illustrated in Figure 1B, the B–D row whisker regions were most clearly parcellated.

In the same cases, rhodamine dextran injections into SpVi (Fig. 1C), which diffused into caudal SpVo and rostral SpVc, produced anterograde labelling in the thalamus (Fig. 1D; adjacent section to that shown in Fig. 1B) that differed in focus and pattern from that of the PrV projection. While SpV's projections to VPM were also patchy and exclusively contralateral, no somatotopic pattern could be discerned. SpV's most robust projections were to extra-barreloid thalamic regions, including the VPM shell that encapsulates the barreloid area (Figs 1 and 2), a caudal and ventral region of VPM that lacks barreloids and significant PrV inputs (Figs 5 and 7), PO (Figs 1, 2 and 5), nucleus submedius (Fig. 3) and zona incerta (Fig. 4). Within the barreloid portion of VPM, SpV projections were sparse relative to those from PrV, and most terminal labelling occurred in the peripheral fringes of whisker-related patches and in inter-barreloid regions (Figs 5–7). All of these projections were totally contralateral, except for the submedius projection, where a significant ipsilateral input was revealed (Fig. 3, left).

These observations suggest different foci of the PrV and SpV projections to the thalamus, even in thalamic nuclei known to receive convergent inputs from PrV and SpV, such as VPM. The complementary nature of these two projections was most readily appreciated with anterograde double-labelling methods, as illustrated in Figures 5–7. When the SpV and PrV projections are visualized simultaneously under fluorescent and bright-field optics, respectively (Figs 5 and 6), it can be seen that PrV fibres were concentrated within and defined the barreloid region; whereas SpV fibres in the barreloid region were preferentially distributed in the outermost fringes of individual barreloids or in PrV fibre-poor regions that will be referred to as inter-barreloid 'septae'. The concentration of SpV terminal swellings in outer-lying portions of single barreloids is perhaps better seen in sections where the anterogradely transported dextran in SpV fibres has been heavy metal-intensified to produce a black label, and the CTB in PrV fibres has been revealed with a brown label (Fig. 7).

A diversity of SpV axon morphologies in the thalamus is also evident in Figure 6. In the shell region near the rostral pole of VPM (Fig. 6A, top left) there were large and medium-sized terminals and few small terminals. Near the caudal pole of VPM (Fig. 6B, bottom right) there were numerous very fine terminals and relatively few large and medium-sized terminals. Even within the barreloid region, a wide array of terminal and arborization types was seen, ranging from small and diffuse to large and grape-like. This is perhaps best appreciated in immunohistochemically stabilized dextran preparations, as shown in Figure 8. Note the differing fibre and bouton sizes within both VPM and PO, as well as the differing arbor shapes within VPM, ranging from clustered and circumscribed to 'stringy' and somewhat tortuous.

Given the above-described finding that SpV fibres project preferentially to 'extra- barreloid' regions of VPM that display a paucity of inputs from PrV, the following question arises: should those shell and septa regions of VPM receiving primarily SpV inputs be considered part of PO, or of some other matrix-like nucleus? A number of observations are relevant to this question. First, antisera to parvalbumin and calbindin have been shown to clearly delineate nuclear borders in and around the ventrobasal complex in the monkey, as well as regions receiving PrV and SpVc inputs (see Rausell and Jones, 1991a, b; Rausell *et al.*, 1992, for data and references). The staining patterns shown in Figure 9 indicate that while VPM, VPL and PO display differing patterns and densities of immunoreactivity for calcium-binding proteins, there are no portions of VPM that stain similarly to PO, save for the SpV-defined shell region. Second, within VPM proper, regions containing patches of SpV terminals did not display diminished levels of parvalbumin immunoreactivity (Fig. 10), nor did they display heightened calbindin staining (Fig. 9). Third, these impressions regarding the homogeneity of the VPM neuropil were confirmed by analysis of other cases processed for acetylcholinesterase or cytochrome oxidase activity, or for Nissl substance and myelin (not illustrated). In these histological materials, no portion of VPM displayed PO-like staining patterns, although in most of the cytochrome oxidase-stained sections whisker-related patches were demarcated by cytochrome-poor septae, as described by Land and Simons (1985). Cytochrome-revealed patches appeared to correspond to the patchy PrV projection to VPM.

Regarding the staining in the thalamus produced by antisera to calcium-binding proteins, other observations were made that relate to previous reports in the monkey by Rausell and Jones (1991a, b). In the rat, parvalbumin-immunoreactive cell bodies were observed only in the thalamic reticular nucleus (Fig. 9) and the zona incerta (Fig. 4); terminals were heavily stained in VPM, VPL and the thalamic ventrolateral and ventromedial nuclei, with a paucity of terminal labelling in PO and the nucleus submedius (Fig. 9). Figure 11 illustrates the absence of parvalbumin-positive cell bodies in VPM, as well as dense terminal staining in VPM that outlined unlabelled cell bodies. A whisker-related staining pattern was only clearly delineated in the dorsalmost sections of VPM (Fig. 9E), and this patterning was less obvious than that seen with cytochrome oxidase or when the PrV projection was labelled with anterograde tracers (Figs 1 and 7). Calbindin immunoreactivity was, to a limited extent, complementary to the above-described parvalbumin pattern. Labelled cell bodies were seen in all thalamic nuclei, save for

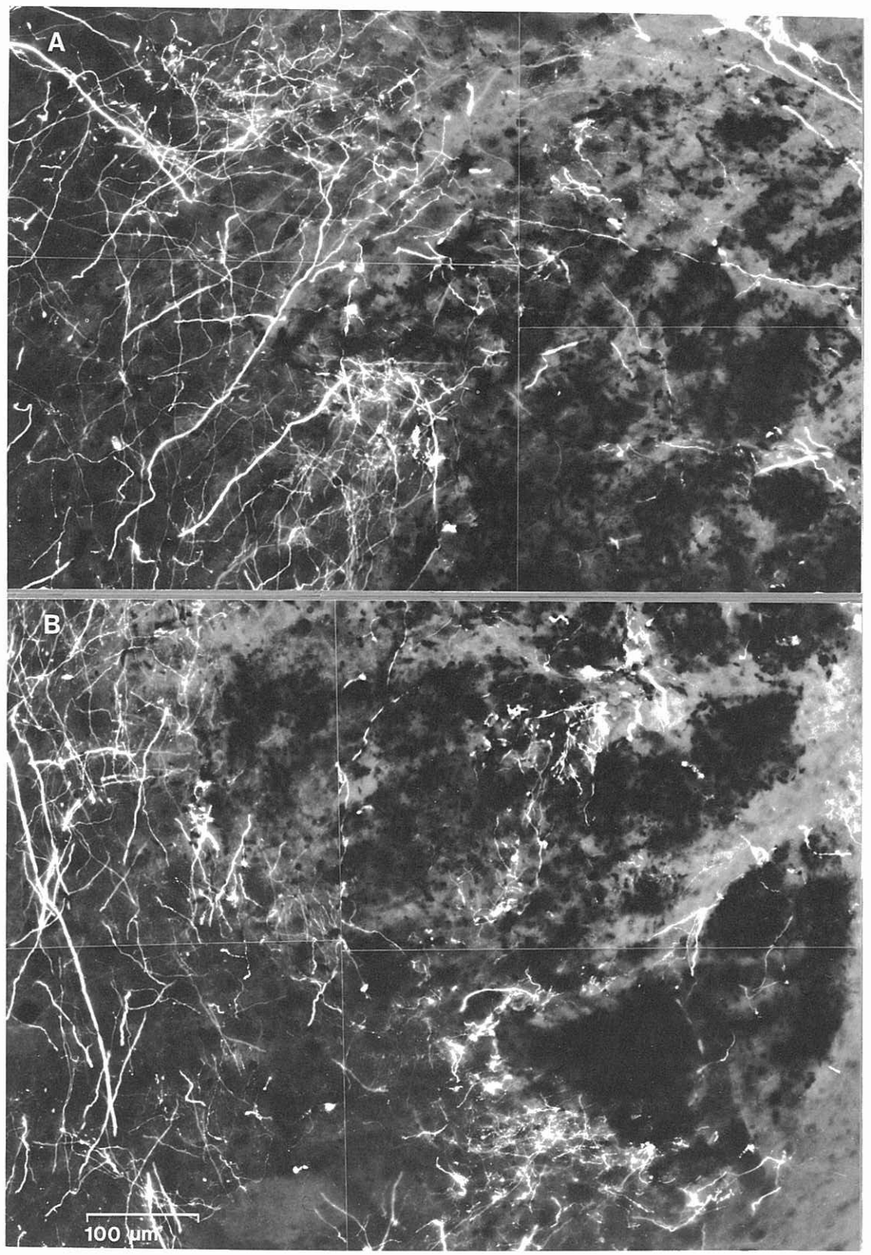

FIG. 6. A more detailed view of those portions of the right PO and dorsal VPM outlined in Figure 5b, showing the differential foci of rhodamine dextran-labelled SpV inputs (white) and CTB-labelled PrV inputs (black). The latter define the VPM barreloid region. A and B show rostral and caudal areas, respectively. See Figure 5 for conventions and Figure 1 for injection sites.

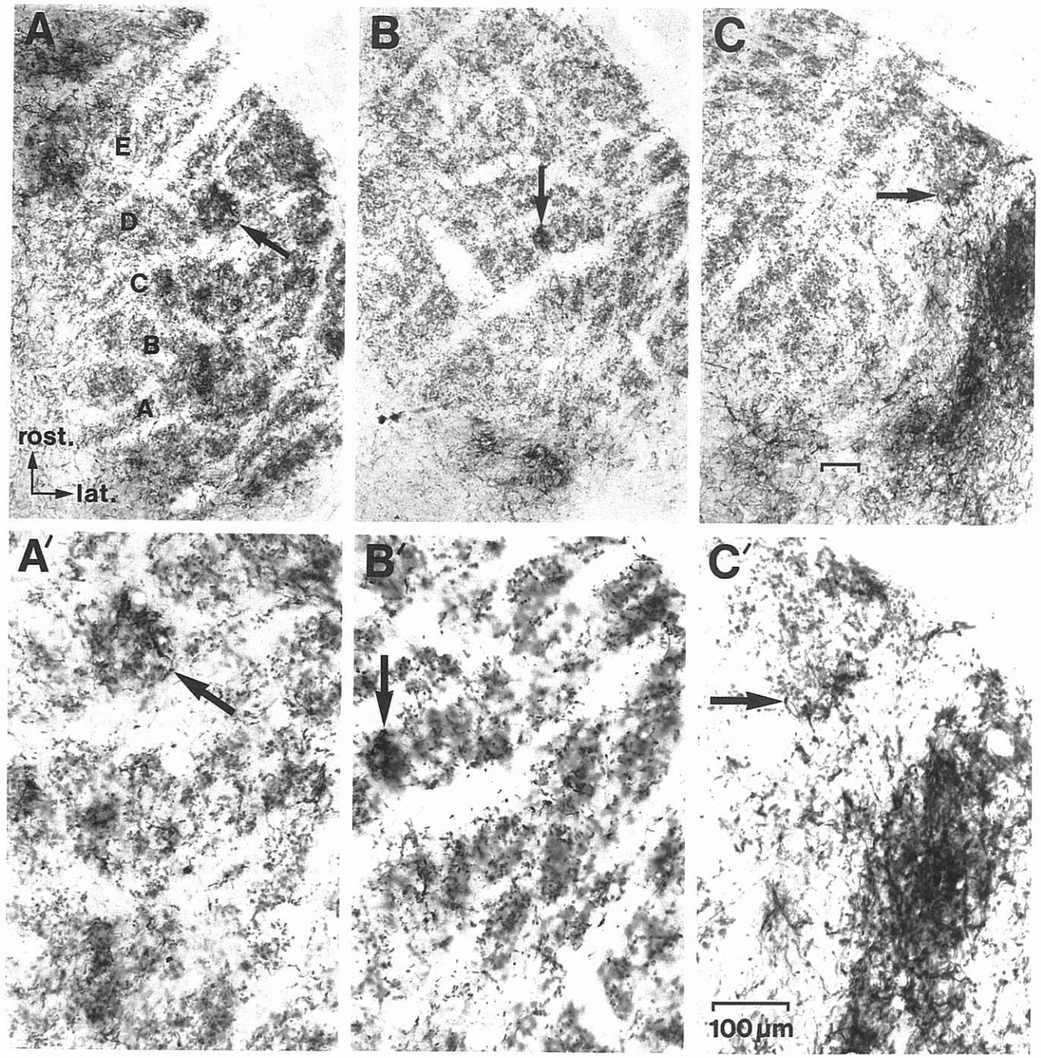

FIG. 7. Bright-field photomicrographs of other horizontal sections from the case shown in Figure 5 that were processed immunohistochemically to render dextran-labelled SpV fibres in black and CTB-labelled PrV fibres in brown. Aggregates of brown fibres define the barreloid pattern in VPM; whisker-related rows are labelled A–E in a dorsal section shown in panel A. B and C are from successively more ventral levels. Arrows are placed at corresponding points in three matching pairs of low- (top) and high-(bottom) magnification photos, as in A and A′, etc. The 100 μm calibration in C applies to A and B as well; C′ also applies to A′ and B′. Note that SpV inputs are preferentially distributed in the peripheral fringes of individual barreloids (arrows in A–C), or in a posteroventrolateral portion of VPM that lacks barreloids and significant inputs from PrV (C).

the reticular nucleus, although cells were most weakly stained in VPM. However, calbindin-positive fibres were sparse in thalamus, although the small number of labelled terminal swellings were quite prominent. In VPM (Fig. 11), calbindin-positive cells and fibres did not correspond spatially in any obvious way to the parvalbumin staining pattern or the pattern of anterogradely labelled SpV or PrV projections.

Experiment 2

Seven fibres in the medial lemniscus were physiologically characterized, impaled and labelled sufficiently with HRP to permit reconstruction of their thalamic terminations. Five of these are drawn in Figures 12 and 13, and illustrated in Figure 14. Six of the seven responded with short-latency, high-frequency following electrical stimulation of PrV; one

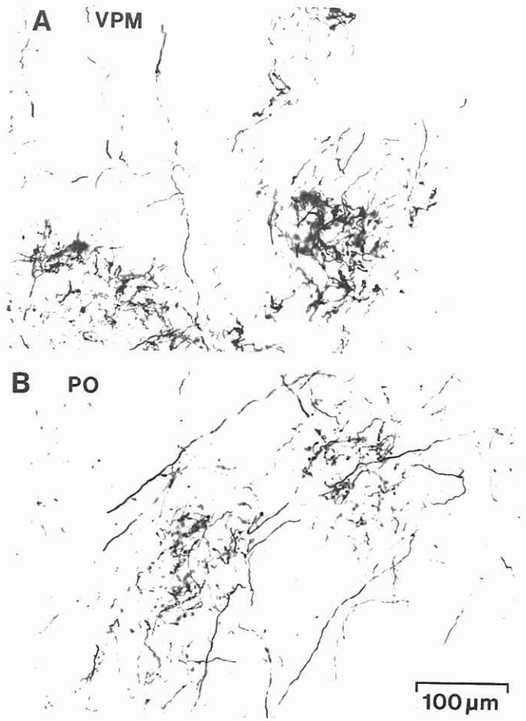

FIG. 8. Bright-field photomicrographs from a 40 μm thick horizontal section showing examples of terminal arbors in the right, dorsal barreloid region of VPM (A) and the right PO (B), which were labelled immunohistochemically by rhodamine dextran injections in the left SpV. The bottom left portion of A is part of the VPM 'shell'. Rostral is up; medial is left.

responded similarly to SpVi stimulation. They all responded to deflection of either a single whisker or a small group of guard hairs. They appeared to have, for the most part, similarly shaped arbors in VPM. None branched in the diencephalon en route to their exclusive site of termination in VPM, where highly localized terminal aggregates were formed in a somatotopic manner matching that of VPM cells (Waite, 1973; Rhoades *et al.*, 1987; Ito, 1988). Areas subtended by the terminal arbor envelopes of single whisker-sensitive fibres never exceeded the areas subtended by their matching barreloids. In this small sample it also appeared that guard hair-sensitive axons had a somewhat more tortuous trajectory and arborization pattern than that of whisker-sensitive axons, but that both groups terminated exclusively within a restricted portion of VPM.

Experiment 3

Figure 15 illustrates a typical set of HRP injection sites in PrV and SpVi and the resultant anterograde labelling in VPM that was processed for electron microscopic analysis. Labelled PrV terminals formed synaptic contacts with unlabelled VPM somata (Fig. 16a and b) and dendrites (Fig. 16c–e). Labelled boutons contained numerous round synaptic vesicles and formed asymmetrical synaptic contacts most frequently with small dendritic spine-like appendages, although they also made synaptic contacts with dendritic shafts. SpV terminals were qualitatively indistinguishable from PrV terminals in their ultrastructural appearance and postsynaptic associations (Fig. 17).

Quantitative analysis of seven cases (Fig. 18) indicated that labelled PrV terminals contacted VPM dendrites with a mean (± SD) diameter of 1.51 ± 0.10 μm; whereas labelled SpV terminals contacted VPM dendrites with a mean diameter of 1.27 ± 0.07 μm. This difference was statistically significant (one-way analysis of variance: $F = 11.6$, $df = 1,6$, $P < 0.01$), reflecting a disproportionate number of PrV terminals in contact with dendrites having a minor axis of >2.5 μm. PrV endings were also more likely to contact VPM cell bodies (11.0 ± 4.2% of all labelled terminals) than those from SpVi (3.0 ± 1.0%, $P < 0.01$), as shown in Figure 19.

Discussion

The results presented here suggest that PrV and SpV have largely complementary projection foci in the thalamus. This conclusion is supported by the following findings: (i) PrV's heaviest projection is to VPM and defines the whisker-related barreloids; (ii) SpV's heaviest projections are to PO, nucleus submedius, zona incerta, the shell region encapsulating VPM, and a ventral and caudal pocket of VPM that lacks barreloids and significant PrV inputs; (iii) SpV's relatively weak inputs to the barreloid region occur most frequently in the outer-lying fringes of single barreloids and in inter-barreloid septa; and (iv) PrV terminals are more likely than SpV terminals to terminate upon VPM somata and its widest dendrites, suggesting that PrV–VPM synapses occur closer to and more frequently upon VPM cell bodies than SpV-VPM synapses. We also found that parvalbumin and calbindin immunoreactivity does not distinguish regions of VPM thalamus containing PrV and SpV inputs. Before discussing the implications of these results, a number of technical aspects must be addressed.

Technical limitations

One of our major findings is a negative one: the thalamic projections of PrV and SpV do not overlap significantly. As with any anterograde tracing study, one must be cognizant of the possibility that a negative result may reflect a technical shortcoming. It is conceivable that this result reflected inadequate transport of tracer from certain regions of, or cell types in, PrV and/or SpV, therein leading to a false negative conclusion. This is unlikely to apply to the present study, however, because complementary projection foci were obtained in all experimental animals with the same and differing tracer permutations, including HRP, CTB, rhodamine and fluorescein dextrans. Moreover, to be included in the analyses, an experimental case had to meet conservative criteria, including large injection sites that spanned the entire transverse dimension of PrV and SpV, intense labelling of fibres arising from all portions of SpVi, and evidence of effective transport to the VPM thalamus. A wide range of postinjection survival intervals was also evaluated and in no case was there evidence of a more robust SpV projection than is described in Results.

In order to fulfil the criteria for effective transport from *all* of SpVi, it became necessary to abandon an original goal of restricting our comparisons to PrV and SpVi projections. Tracer diffusion to SpVc and SpVo routinely occurred in those cases where SpVi was intensely labelled in its entire rostrocaudal extent. Diffusion into SpVc was unavoidable because of the rostrocaudally oblique nature of the SpVi–SpVc transition zone, where previous studies (Yoshida *et al.*, 1991) have documented a large number of thalamic projecting cells. As such, the most appropriate interpretation of the anterograde labelling described here is that it reflects projections from all three SpV subnuclei. Given the similarities in the receptive field properties of thalamic projecting cells in SpVi, SpVo and

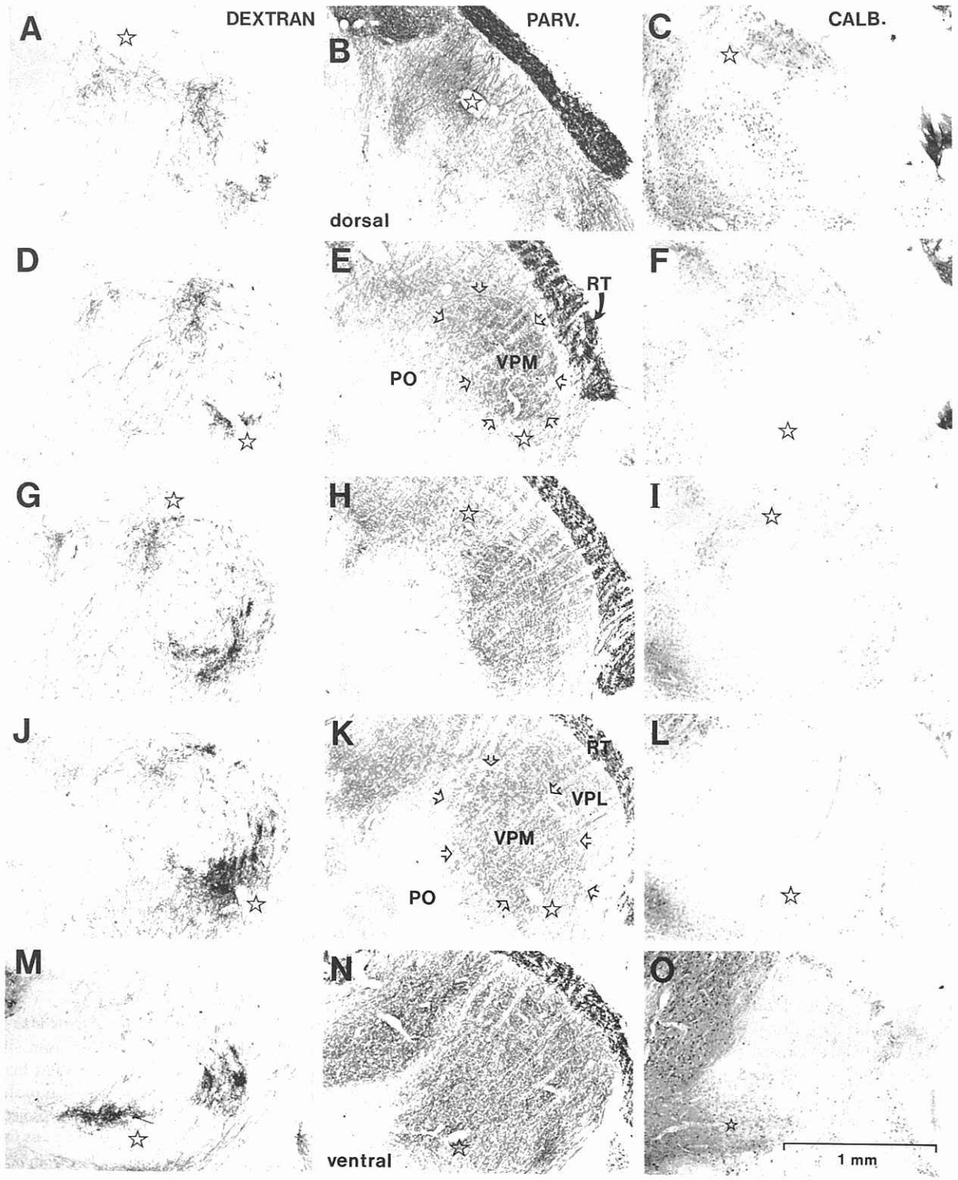

FIG. 9. Bright-field photomicrographs showing rhodamine dextran-labelled SpV projections (A, D, G, J, M) and parvalbumin (PARV; B, E, H, K, N) and calbindin (CALB; C, F, I, L, O) immunoreactivity in a successive series of alternating horizontal sections encompassing the full dorsal (A) to ventral (O) extent of VPM. Stars are placed at equivalent points along identifying blood vessels in each triplet (e.g. A–C) to facilitate comparison of the three staining patterns in adjacent sections. In E and K, the boundaries of VPM are delimited by open arrows. Note that where parvalbumin staining is dense, calbindin staining tends to be weak, but that regions in and around VPM containing SpV inputs do not display reduced parvalbumin immunostaining. Sections shown in A–C and M–O skim the dorsal and ventral borders of VPM, respectively. See Figure 1 for conventions. In each plate rostral is up; medial is left.

the deep laminae of SpVc (see Introduction for references), and their stark contrast with the response properties of PrV cells (Jacquin *et al.*, 1988), the SpV–PrV distinction drawn here is likely to be a meaningful one in physiological terms. A small number of thalamic projecting lamina I cells in rostral SpVc would be included in our SpV injection sites, and these cells do have physiological properties that are distinct from

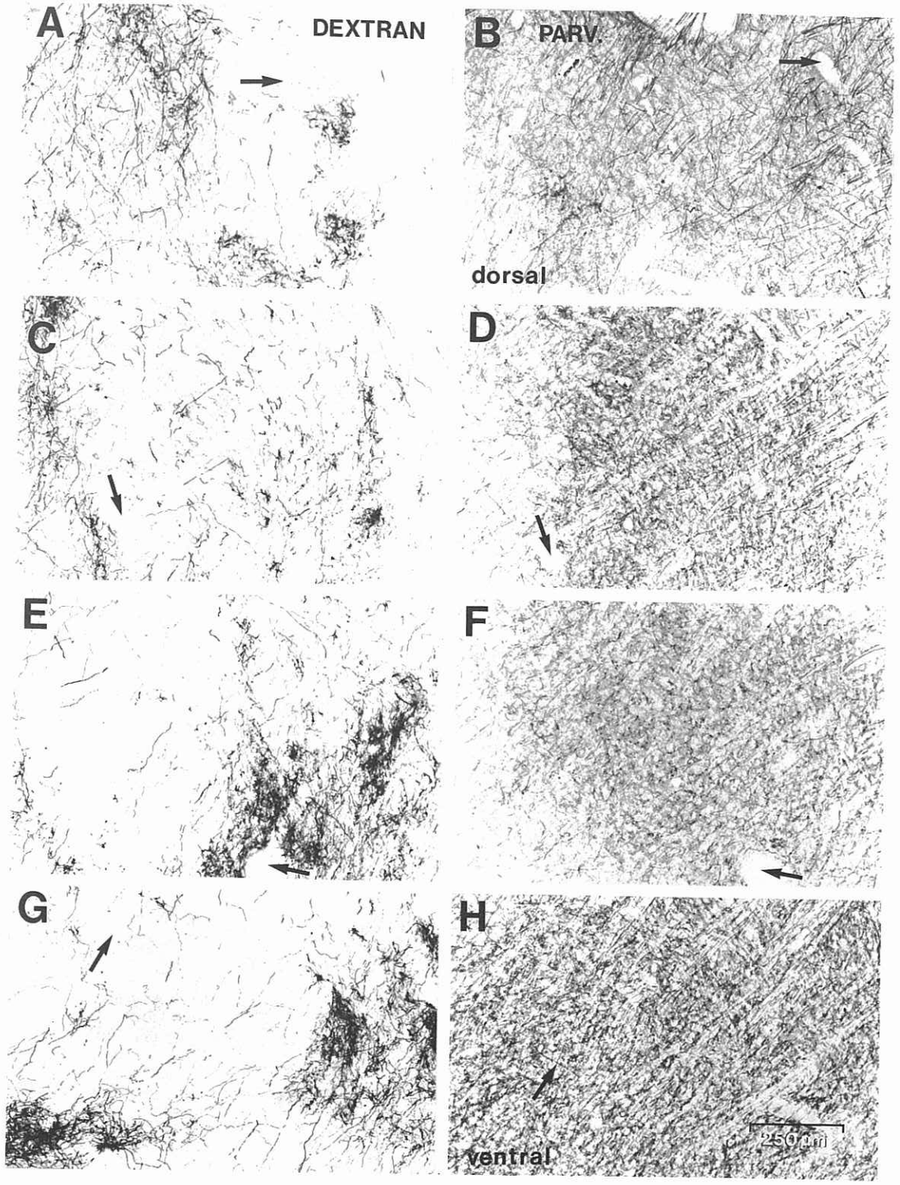

FIG. 10. A more detailed view of rhodamine dextran-labelled SpV projections (A, C, E, G) and parvalbumin (PARV.; B, D, F, H) immunoreactivity in adjacent pairs of horizontal sections spanning dorsal (A) to ventral (H) VPM. Arrows are placed at equivalent points in each pair (e.g. A, B) to facilitate comparison of the two staining patterns in adjacent sections. Note the non-complementary nature of these two markers, as well as their inability to reveal well-defined whisker-related patterning in VPM.

SpVi and SpVo cells (Renehan *et al.*, 1986; Jacquin *et al.*, 1989; Jacquin and Rhoades, 1990). As such, it is prudent to consider our results as reflective of the 'paralemniscal' SpV pathway, recognizing that the vast majority of the terminal labelling arises from low threshold mechanoresponsive cells in SpVi (Jacquin et al., 1986a; Jacquin, 1989).

Another limitation pertains to the small sample of fibres stained with HRP after physiological classification. However, because of the pivotal role of these fibres in establishing thalamic receptive fields (see below),

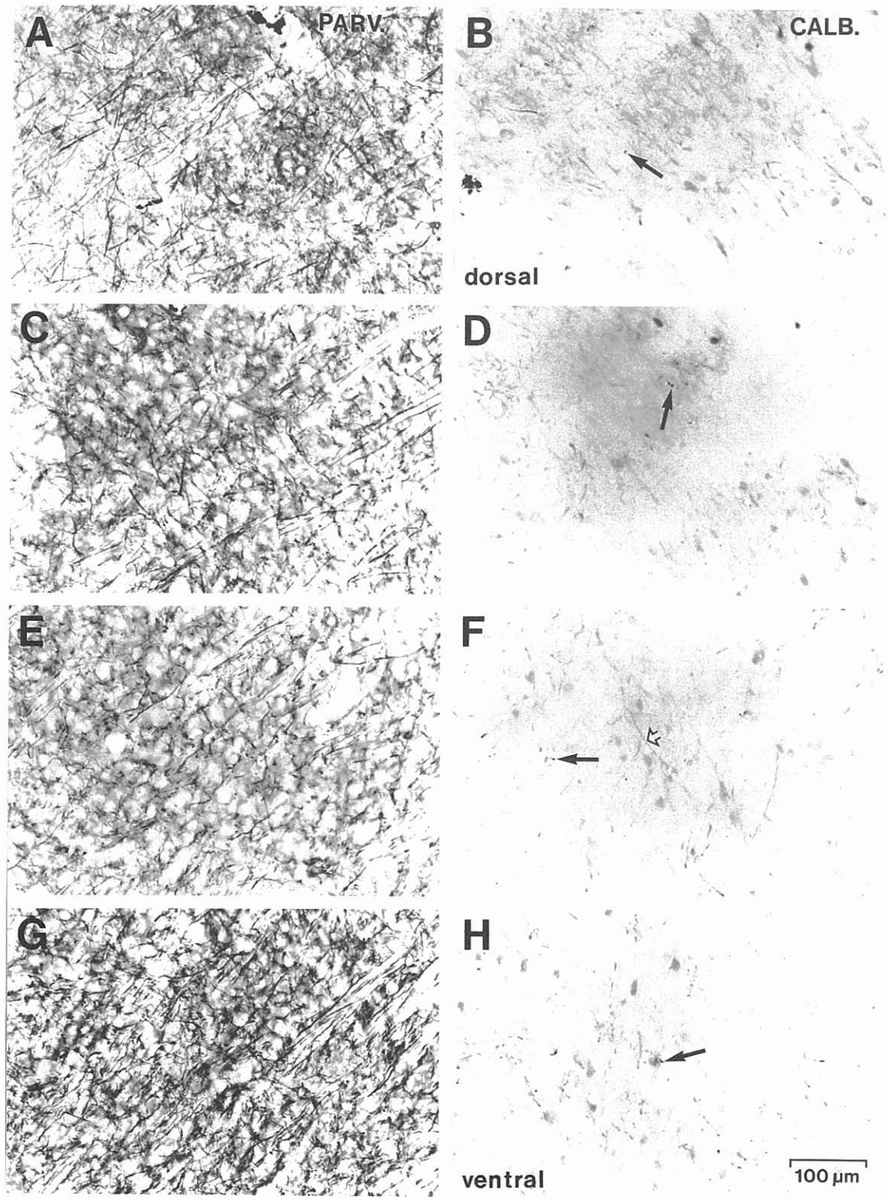

FIG. 11. Parvalbumin (PARV.; A, C, E, G) and calbindin (CALB.; B, D, F, H) immunoreactivity in adjacent pairs of horizontal sections spanning dorsal (A) to ventral (H) VPM. Note the absence of parvalbumin-positive cell bodies, and the weakly stained calbindin-positive somata. Although calbindin darkly stains terminals (filled arrows) and fibres (open arrow), they are few in number and bear no orderly distribution relative to parvalbumin-stained elements.

even a limited database is useful. If the axons reconstructed here are representative of the V-thalamic population, their circumscribed arbors with dimensions that do not exceed that of a single barreloid and their singular thalamic target (VPM) are essential features in interpreting the physiological properties of thalamic cells. Clearly, further study is warranted at the single-axon level.

A final limitation inherent to our conclusions regarding the synaptic organization of PrV and SpV projections in VPM reflects the assumption

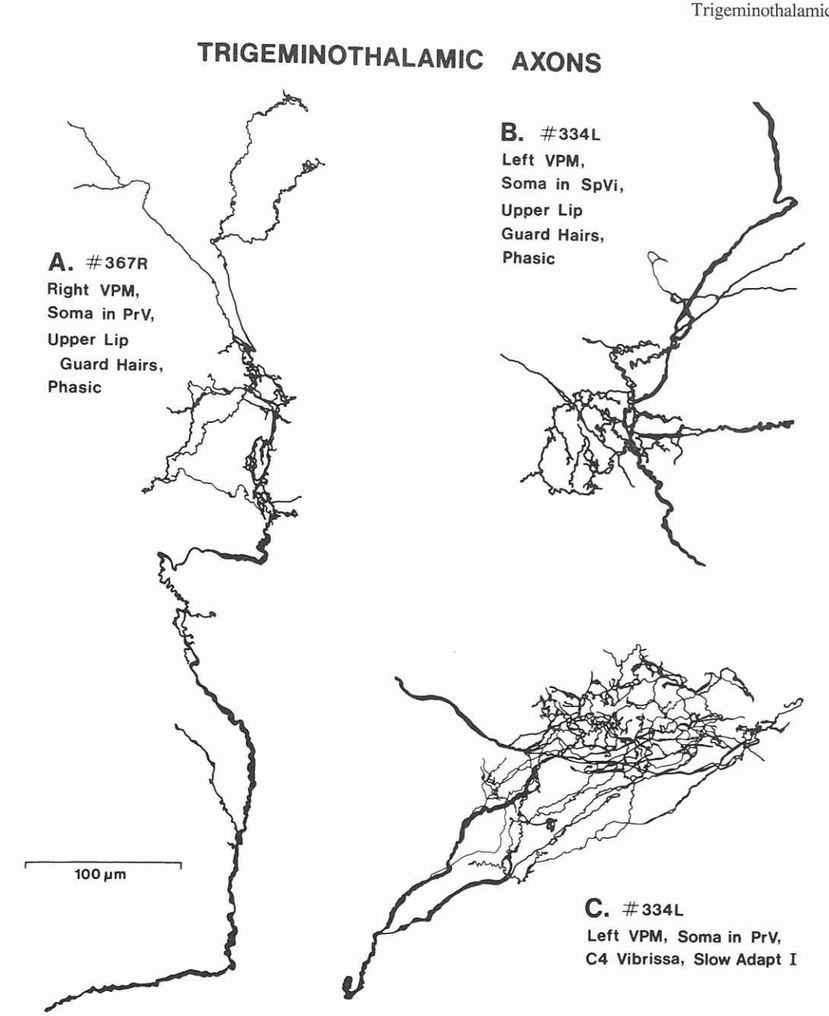

FIG. 12. Reconstructions in the transverse plane of the thalamic arbors from 2 PrV cells (A, C) and one SpVi cell (B). Their axons were injected with HRP in the medial lemniscus subsequent to physiological characterization. Axon A responded in a rapidly adapting fashion to sustained displacement of a small patch of guard hairs on the left upper lip. Its response latency to contralateral PrV shocks was 0.5 ms and it discharged to each cycle of a 200 Hz shock train. SpVi shocks also activated the axon, but the response latencies and absence of high frequency following were indicative of synaptic activation. Axon B had a similar receptive field to that of A on the right upper lip, and responded to each cycle of an SpVi shock train with a 1.2 ms latency. For axons A and B there was no evidence for coding for direction, velocity or magnitude of hair displacement, nor spontaneous activity. Axon C displayed slowly adapting type I firing (Jacquin *et al.*, 1986c) to sustained displacement of the right C4 whisker in the rostral and dorsal directions, increasing spike numbers to increasing distances of hair displacement, and no spontaneous activity. Its latency to PrV shocks was 0.6 ms. Case numbers are provided for comparison with Figure 14.

that a thin VPM dendrite is one that occurs at a relatively long distance from the cell body (distal) and a thick VPM dendrite is one that is more proximal to the cell body. Such a relationship was derived from prior reconstructions of intracellularly labelled VPM cells in the rat (Harris, 1986; Chiaia *et al.*, 1991b). It must be emphasized that a dendrite's minor axis only correlates with its absolute distance from the cell body and numerous exceptions exist. However, in considering the relationship between VPM dendritic width and electrotonic distance from the somata (Koch et al., 1983), our assumption is probably a valid one in physiological terms. Though more challenging technically, a more direct assessment of the relative spatial positioning of PrV and SpV terminals on VPM dendrites would require that the dendritic trees of single VPM cells be reconstructed in their entirety.

Divergence, convergence and patterning of PrV and SpV projections

Prior studies have shown that PrV and SpV projections to the thalamus have divergent and convergent properties. Insofar as major differences

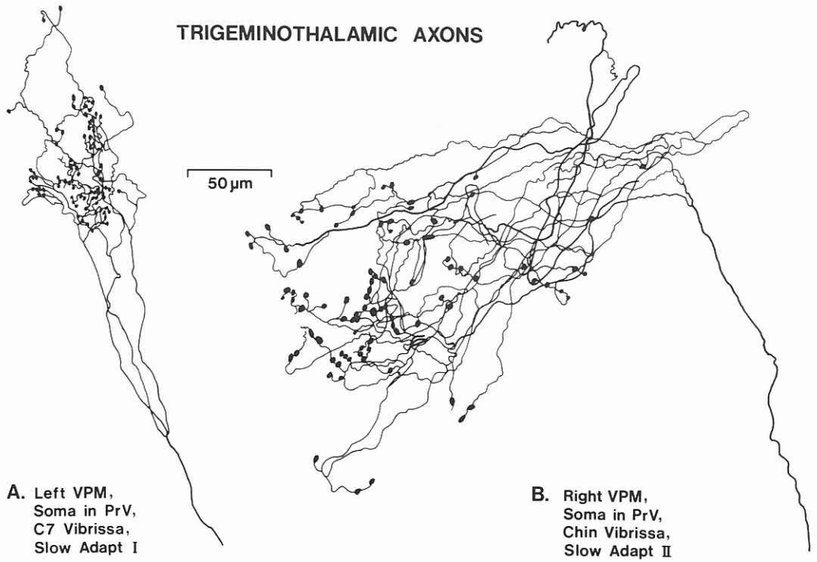

FIG. 13. Additional transverse reconstructions of identified V-thalamic axons. Axon A responded in a slowly adapting type I fashion to sustained displacement of the right C7 whisker. There was no evidence for direction, velocity or magnitude sensitivity, nor was it spontaneously active. Latency to high-frequency and contralateral PrV shocks was 0.5 ms. Axon B responded in a slowly adapting type II fashion to sustained displacement of one left chin whisker. There was no evidence for direction or velocity sensitivity or spontaneous activity. It was sensitive to the degree of whisker displacement. Its latency to high frequency and contralateral PrV shocks was 0.5 ms.

exist in thalamic organization between rodents, cats and monkeys, our discussion of these issues will be largely restricted to work done in rodents (see Jones, 1985; Ralston *et al.*, 1988; Rausell *et al.*, 1992, for discussion of the monkey and cat). Many of the observations reported here are consistent with prior reports. Anterograde and retrograde labelling experiments have demonstrated significant PrV (Erzurumlu *et al.*, 1980; Bates *et al.*, 1982; Peschanski, 1984; Chiaia *et al.*, 1991a) and SpV (Erzurumlu and Killackey, 1980; Peschanski, 1984; Chiaia *et al.*, 1991a; Yoshida *et al.*, 1991) projections to VPM, and we concur that PrV has a greater input than SpV to VPM. Results presented here are also in line with prior indications that the most substantive V brainstem input to PO arises from SpV (Chiaia *et al.*, 1991a), and that the nucleus submedius and zona incerta receive major inputs from SpV (Peschanski, 1984; Roger and Cadusseau, 1985; Shammah-Lagnado *et al.*, 1985; Ma *et al.*, 1988; Yoshida *et al.*, 1991; Nicolelis et al., 1992). These inputs should be major contributors to the low-threshold orofacial receptive fields of cells in VPM (see below for detailed discussion), PO (Chiaia *et al.*, 1991b; Diamond *et al.*, 1992a, b), submedius (Dostrovsky and Guilbaud, 1988; Miletic and Coffield, 1989) and zona incerta (Nicolelis *et al.*, 1992).

The new information provided here is as follows. First, anterograde tracing experiments indicate that the projection from PrV to VPM is patterned in a whisker-related manner, and that this pattern is most distinct in dorsal VPM. This result was not surprising, in the light of prior metabolic, histochemical and retrograde staining indications that VPM cells are patterned (reviewed in Land and Simons, 1985; Killackey *et al.*, 1990; Woolsey, 1990; Diamond *et al.*, 1992a). However, a demonstration of patterned V inputs to VPM has not been published. The paucity of somatotopic patterning in prior demonstrations of V-thalamic projections probably reflects the fact that VPM has been routinely presented in the transverse plane, therein offering only a limited portion of the somatotopic map in a single section. Here, horizontal sections were processed so as to view the complete map, therein revealing clearcut whisker-related segmentation in the PrV–VPM projection. In alternate sections, SpV projections were not arrayed in whisker-related patterns in any of its targets.

Second, it would appear that SpV projects more heavily to PO than to VPM (see especially Fig. 2). This interpretation differs from that made by Chiaia *et al.* (1991a), who counted the numbers of retrogradely labelled cells in SpVi following fluorescent tracer deposits in VPM and PO. In that study, 75% of the labelled SpVi cells projected to VPM and only 17% projected to PO. The contrasting results between the two studies most likely reflects the fact that Chiaia *et al.* used 'quite small' injections to prevent tracer diffusion between VPM and PO, as well as the fact that PO is a larger nucleus than VPM and larger volumes of tracer would be required to adequately represent the PO projection.

Third, axon arbor morphologies in PO and VPM of SpV origin do not appear to differ appreciably (see especially Fig. 8). This conclusion differs from that of Chiaia *et al.* (1991a), who reported that anterogradely labelled collaterals had more 'widespread' arbors in PO than in VPM, irrespective of the V brainstem subnucleus of origin. Our intra-axonal staining data, however, concur with the retrograde double-labelling results of Chiaia *et al.* in that no stained axon branched to terminate in both VPM and PO.

Fourth, and perhaps most importantly, anterograde double-labelling experiments suggest only limited convergence of the PrV and SpV projections to VPM. This result was surprising because, except for one report in the monkey where SpVc and PrV were shown to have largely non-overlapping, complementary terminations in VPM (Rausell and Jones, 1991b), all available anatomical and electrophysiological evidence

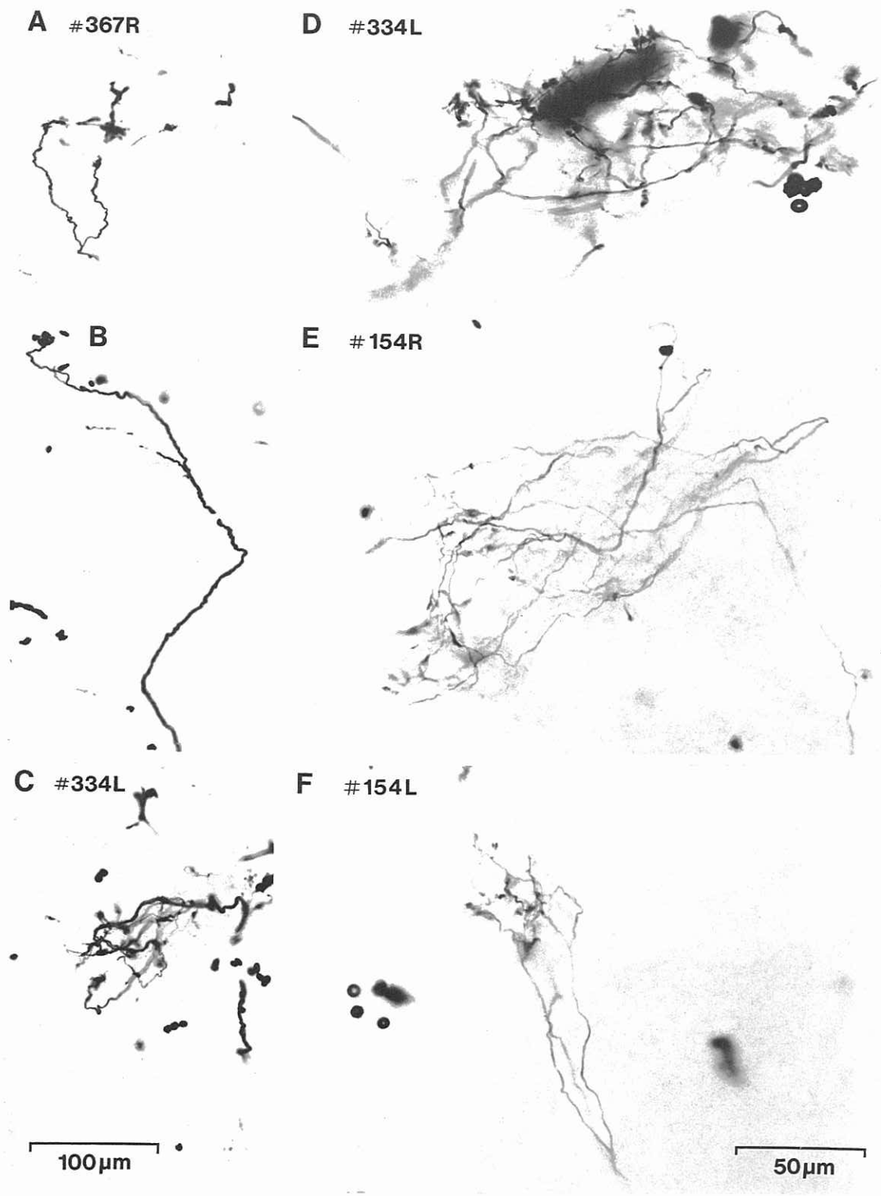

FIG. 14. Bright-field photomicrographs of transverse sections through VPM illustrating the morphologies of V-thalamic axons reconstructed in Figures 12 and 13. Case numbers are provided to aid comparisons. A and B were taken from adjacent sections drawn in Figure 12A, C from 12B, D from 12C, E from 13B, and F from 13A. The calibrator in C applies to A and B as well; the calibrator in F also applies to D and E.

in rats pointed towards robust PrV–SpV convergence in VPM. Indeed, in summarizing their and others' analyses of the PrV and SpVi projections to VPM in the rat, Chiaia *et al.* (1991b) state that 'one is most struck with their similarities and the fact that both converge … [and that both] terminate in a restricted, topographic and almost certainly overlapping fashion'. This is exactly the conclusion we drew from our preliminary single-labelling experiments. However, it would appear that the PrV inputs are most robust in, and define, the whisker-related barreloids,

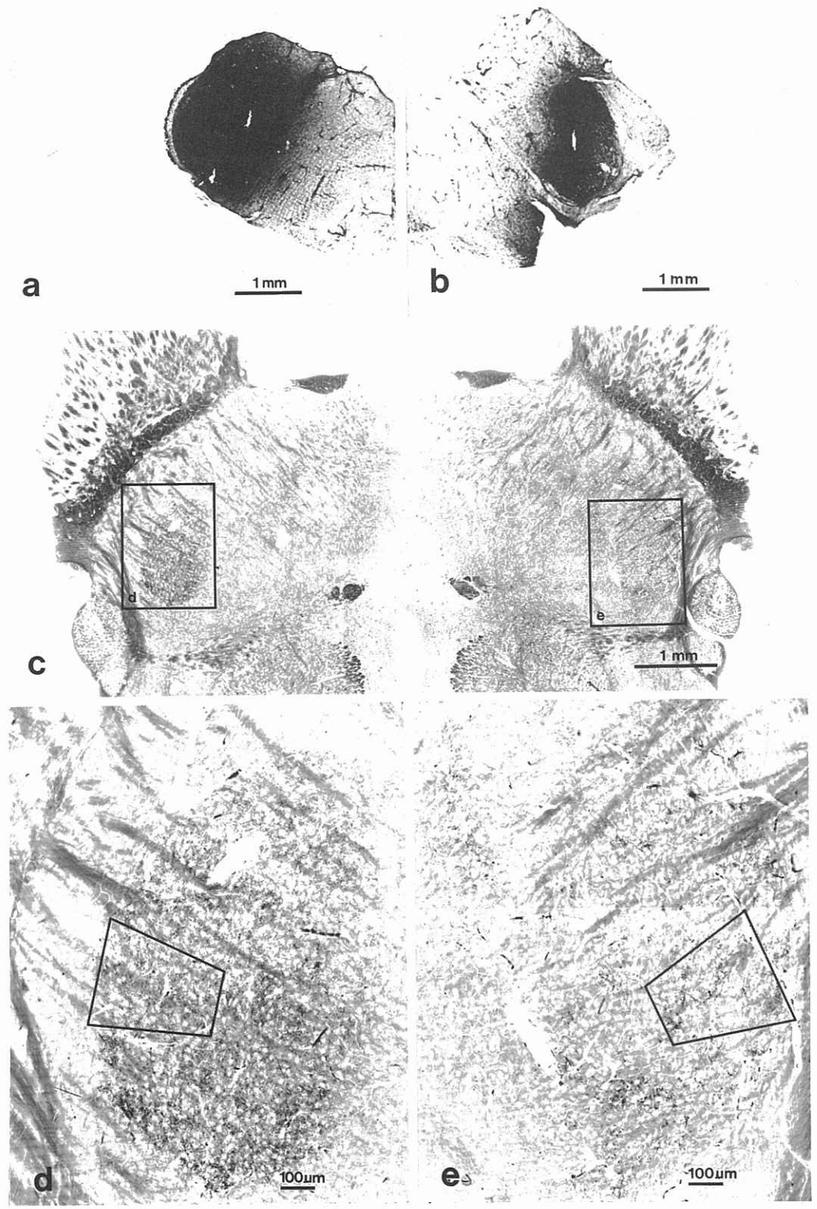

FIG. 15. Bright-field micrographs of representative HRP injection sites and the resultant terminal labelling used to study the pre- and postsynaptic organization of PrV and SpV projections to VPM. Panels a and b show transverse sections through the maximum cross-sectional extent of the injection sites in SpVi and PrV, respectively; cobalt-intensified diaminobenzidine reaction. Panel c shows a horizontal section containing labelled PrV (right) and SpVi (left) inputs to the left and right VPM, respectively; TMB reaction stabilized with diaminobenzidine and cobalt. The boxed regions in c are shown at higher magnification in d and e. The regions outlined in d and e were re-embedded, resectioned and studied in the electron microscope.

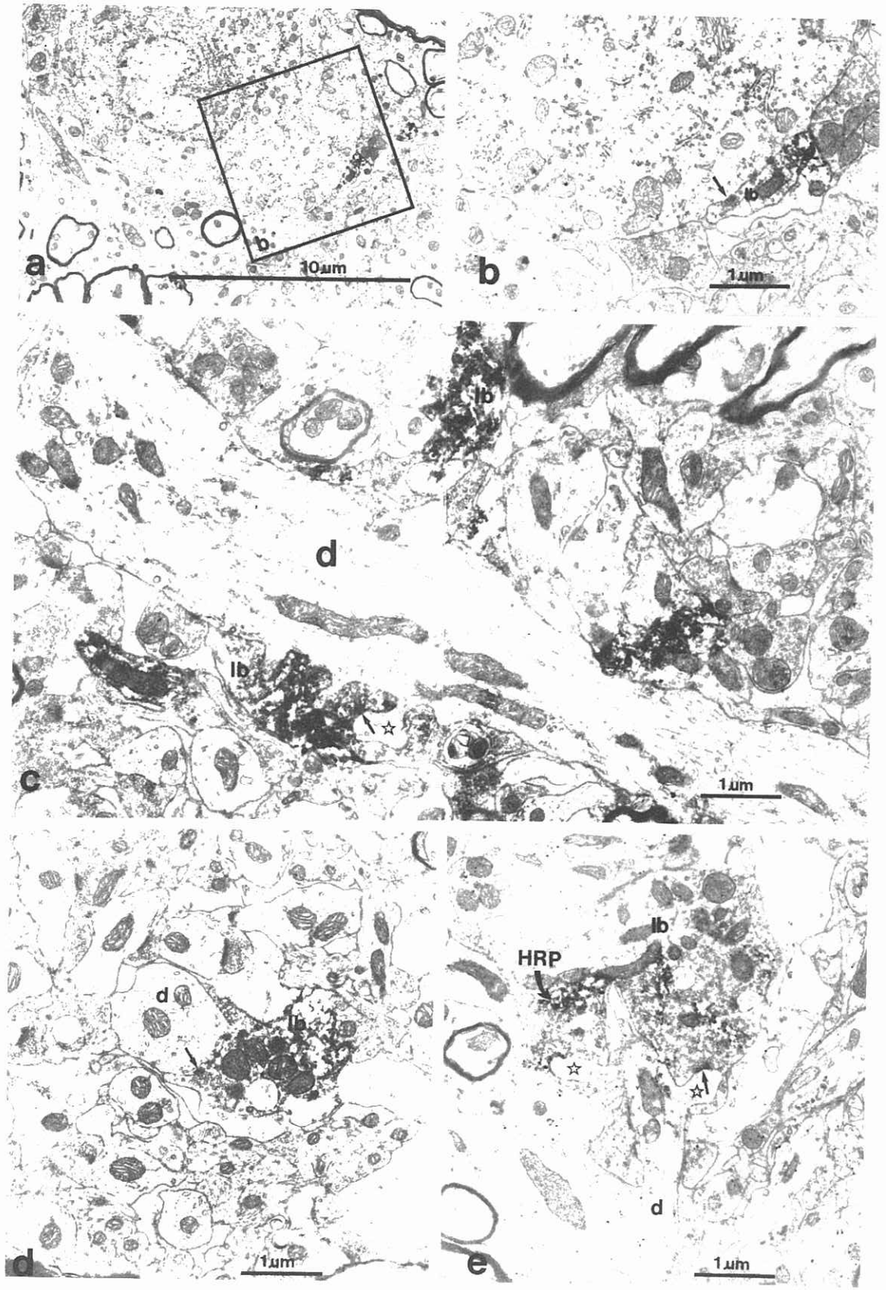

FIG. 16. Electron micrographs of HRP-labelled terminal boutons (lb) from *PrV* forming axosomatic (a, b) and axodendritic (c–e) synaptic contacts in the left VPM. Panel a shows at low magnification a VPM cell body in contact with a labelled bouton; the boxed region is shown at higher magnification in b, indicating numerous synaptic contacts (arrow) with the unlabelled cell. Labelled boutons also form synaptic contacts with large (c), medium (d) and small (e) dendrites. Labelled boutons contain numerous synaptic vesicles and form asymmetrical synaptic contacts (e, straight arrows) that are associated mainly with spine-like cytoplasmic appendages extending from somata and dendrites (stars in c and e). Synaptic contacts also occur directly on dendritic shafts (indicated by d). HRP, reaction product.

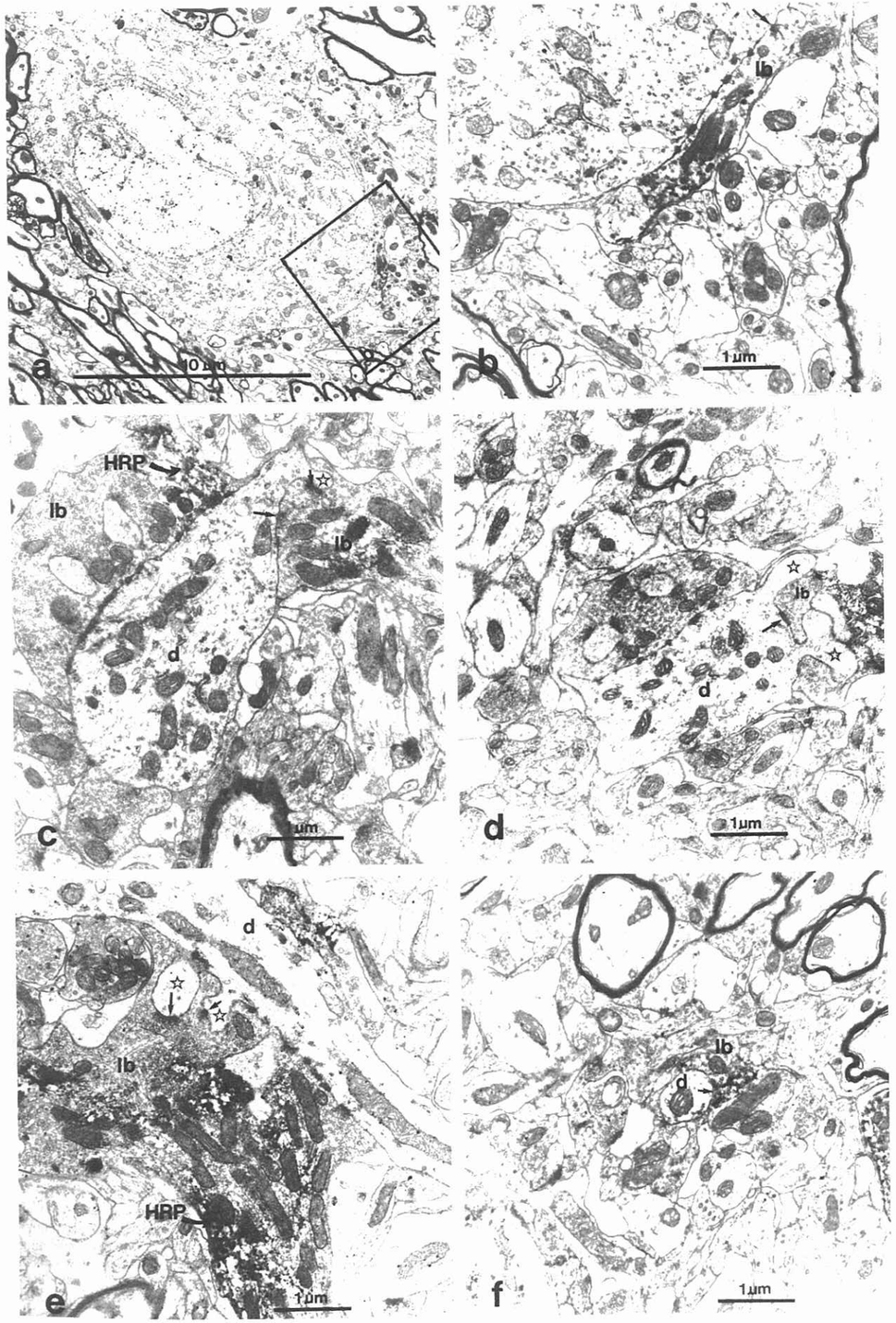

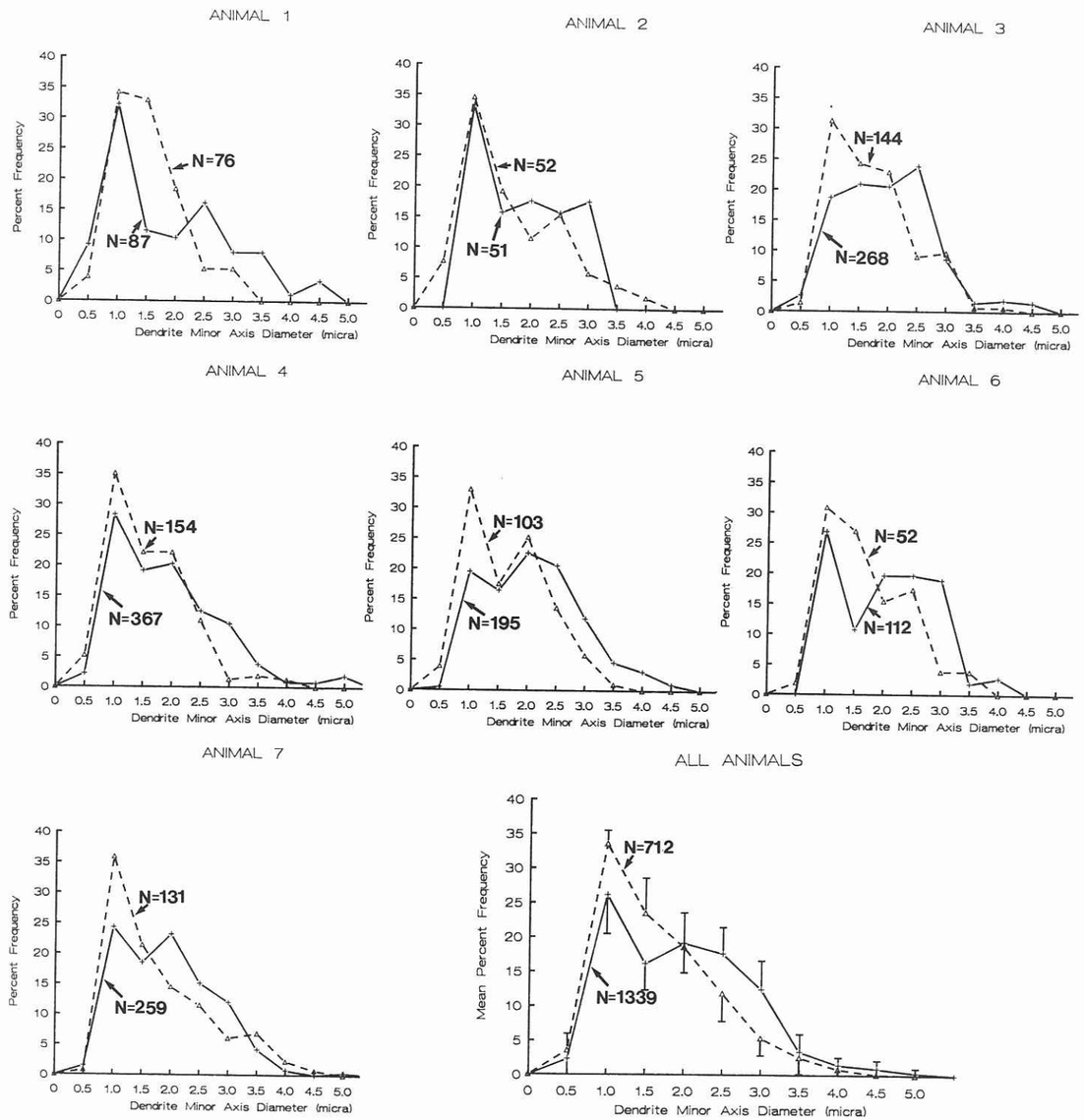

FIG. 18. Size frequency distributions of VPM dendrites (minor axis) receiving synaptic contacts from PrV (+ symbols connected by solid lines) versus SpV (triangles connected by dotted lines). Matching regions of the right (SpV terminals) and left (PrV terminals) VPM were sampled in seven animals displaying robust labelling in VPM. Data are plotted as percentage of the total number of observations by case (ANIMAL 1–7) and as group mean with standard deviation (ALL ANIMALS; bottom right). The numbers of terminals (N) providing measurements of postsynaptic dendrites are also provided for each VPM analysed.

FIG. 17. Electron micrographs of HRP-labelled terminal boutons (lb) from *SpV* forming axosomatic (a, b) and axodendritic (c–f) synaptic contacts in the right VPM from the same case used to illustrate PrV terminals in the left VPM (Fig. 16). See Figure 16 for conventions. Panels a and b show a VPM cell body in synaptic contact with a labelled bouton. Synaptic contacts are also seen between labelled boutons and large (c), medium (d, e) and small (f) dendrites. Labelled boutons are usually very large (c–e), contain numerous densely packed rounded synaptic vesicles (c–e), form asymmetric synaptic contacts (especially in d and e; small arrows), and terminate most often on small dendritic spine-like appendages (stars in d and e) and dendritic shafts (indicated by d).

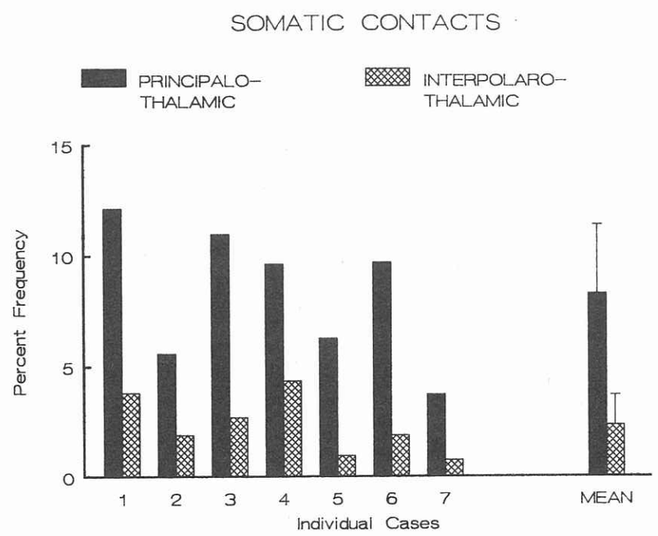

FIG. 19. Frequency histogram of the relative percentages of all labelled PrV (solid) versus SpV (hatched) terminals displaying synapses that do so with VPM cell bodies. Data are plotted as percentage of the total number of observations made in individual cases (ANIMAL 1–7, from Fig. 18) and as group mean with standard deviation (MEAN; right).

whereas the SpV inputs are sparse in the barreloid centres and arborize more significantly within a shell that encapsulates the barreloid field, and within a ventral and caudal invagination of VPM where PrV inputs are sparse. Electron microscopic experiments lend support to these observations in showing that PrV terminals synapse on wide dendrites that are contacted by only a few SpV terminals, and that PrV terminals are more likely to synapse on cell bodies. Although information on VPM dendritic orientation relative to barreloid walls is lacking, these data suggest that SpV disproportionately accesses VPM dendrites in their more distal positions, as has been previously described for dorsal column and spinothalamic inputs to VPL cells (Ma *et al.*, 1986, 1987). As such, our results are consistent with the known organization of the visual thalamus (Stone, 1983), where parallel pathways remain segregated. The failure of prior studies to reveal different termination foci in PrV and SpV projections to VPM in rodents probably reflects limitations in the single-labelling paradigm for revealing fine-grain spatial interdigitation in the V-thalamic parallel pathways.

Parvalbumin and calbindin as markers of PrV and SpV projections?

Prior studies by Jones and co-workers in the monkey (reviewed in Rausell *et al.*, 1992) and Rhoades and co-workers in the rat (Bennett-Clarke *et al.*, 1992) led us (and Diamond *et al.*, 1992b) to some rather straightforward predictions that, if confirmed, would help clarify many unresolved issues. Bennett-Clarke *et al.* (1992) reported that parvalbumin immunoreactivity identifies many thalamic-projecting PrV neurons, the vast majority of which are single whisker-sensitive (Jacquin *et al.*, 1988), whereas calbindin staining marks many thalamic-projecting SpV neurons, the vast majority of which are multiwhisker-sensitive (Woolston et al., 1982; Jacquin *et al.*, 1986a, 1989). Insofar as Rausell and Jones (1991a, b) found that SpVc projects to small-celled, calbindin-positive, 'matrix' components of VPM that lie between and around parvalbumin- and PrV projection-defined, somatotopic 'rods' in the monkey VPM, it seemed likely that the rat VPM would be similarly parcellated and that histochemical compartments could be identified. Our results, however, were inconsistent with these predictions. On the one hand, parvalbumin immunoreactivity failed to stain somata in the rat VPM, unlike the monkey VPM, and this marker provided rather homogeneous terminal staining patterns in the rat VPM, again unlike the monkey VPM. As such, parvalbumin did not optimally demarcate thalamic modules that were demonstrated in adjacent sections with anterograde tracers. On the other hand, calbindin immunoreactivity failed to reveal a matrix-like organization in rat VPM; in fact cells were only weakly stained and darkly stained terminals were sparse. Needless to say, calbindin failed to mark the rat's 'paralemniscal' pathway in and around VPM. These results could be interpreted in a number of ways. Our interpretation is that rat and monkey VPM have different neurochemical properties, although patch/matrix properties can be revealed in both species with anterograde tracers. In the rat, it would appear that calbindin does not mark the majority of SpV–thalamic terminals that have been previously shown (Bennett-Clarke *et al.*, 1992) to be calbindin-positive.

The failure of calcium-binding protein immunoreactivity to reveal intercalated somatotopic modules, matrix and parallel pathways in the rat thalamus does not in any way question their existence. The modular organization of rat VPM is well established, as evidenced by its barreloid organization (e.g. Van der Loos, 1976; Simons and Land, 1985). Moreover, we have documented that parallel pathways are maintained in the rat's thalamus, as well as the existence of an SpV projection-defined matrix in VPM. An alternative view has been presented, however. Diamond *et al.* (1992b) have suggested that a 'matrix' does not exist in the rat VPM, that every neuron is a member of a barreloid, and that the space between barreloids is made up of fibres of passage. They hypothesized that the rat's PO is analogous to the monkey's VPM matrix. The basis for this hypothesis, as presented by Diamond *et al.* (1992b), is sound in all respects, except that it is inconsistent with the presently described SpV matrix-like projection pattern. It just so happens that calbindin immunoreactivity fails to identify a 'matrix' in VPM. An important and yet to be tested hypothesis that will certainly bear upon the utility of the 'patch/matrix' conceptualization of VPM is that cells in 'patch' and 'matrix' have differing physiological properties. Testing of this hypothesis would be facilitated by intracellular labelling of characterized cells and dendritic reconstruction relative to PrV-defined 'patches' and SpV-defined 'matrix'.

Physiological implications

Most accounts of VPM cell receptive fields in the rat indicate a preponderance of single-whisker sensitivity (see Introduction). Insofar as VPM is known to have a major role in establishing principal whisker receptive fields in layer IV cells in the barrel cortex (Simons and Carvell, 1989; Armstrong-James *et al.*, 1991), and the barrel cortex is widely used as a model for CNS information processing (White, 1989), it is important to understand how VPM receptive fields are synthesized. This issue remains enigmatic for a number of reasons, the most significant of which are as follows. It is widely held that PrV and SpV inputs have overlapping and convergent inputs in VPM, yet the multiwhisker receptive fields of thalamic-projecting SpV cells (Jacquin, 1989) are not reflected in most accounts of VPM receptive fields. The latter more faithfully recapitulate the single-whisker receptive fields of thalamic-projecting PrV cells (Jacquin *et al.*, 1988). It is only when PrV inputs are ablated or under light anaesthesia that most VPM cells display SpV-like multiwhisker inputs (Rhoades *et al.*, 1987; Friedberg *et al.*, 1993a, b). To account for the different effectiveness of these two parallel pathways in activating VPM cells, Rhoades *et al.* (1987) hypothesized that SpVi fibres end on more distal portions of VPM dendrites than those from PrV and that, by ablating PrV, normally ineffective SpV inputs become effective in discharging VPM cells. In the present study, we have taken the first step in testing this hypothesis and find that VPM terminals originating in PrV are more likely to synapse on the thickest dendrites and somata than those taking origin in SpV. Perhaps more importantly, we have found in double-labelling experiments that PrV and SpV inputs to VPM are more spatially segregated than would be predicted from prior studies of these parallel pathways. In fact, our impression is that they are complementary; one targets the barreloids, the other preferentially targets extra-barreloid regions of VPM. Therefore, it is not surprising that VPM cell receptive fields are most similar to those of PrV cells because individual whisker-related barreloids are largely devoid of SpV inputs. Our results would predict that the minority of VPM cells that do have multiwhisker receptive fields are located in extra-barreloid regions, or on rare occasions, in the outermost fringes of single barreloids or between barreloids.

How then does one reconcile the present results with those of more recent studies showing that multiwhisker convergence is detectable in most VPM cells under specific recording conditions? Simons and Carvell (1989), Armstrong-James and Callahan (1991) and Friedberg *et al.* (1993b) all reported a high percentage of VPM cells with multiwhisker receptive fields in rats anaesthetized with fentanyl or lightly anaesthetized with urethane. The Friedberg *et al.* study is particularly relevant in having demonstrated an immediate decrease in VPM whisker receptive field size in lightly anaesthetized rats after SpV lesions. Similarly, Chiaia *et al.* (1991b) found that EPSPs could be elicited in most VPM cells by electrical stimulation of either PrV or SpVi and that an average of 2.7 whiskers produced EPSPs in VPM cells that on average were discharged by only 1.4 whiskers.

Thus, both supra- and subthreshold multiwhisker inputs are readily demonstrable in VPM cells. There are four non-mutually exclusive ways in which these receptive fields could be synthesized. First, corticothalamic inputs may impact on VPM receptive field size in a manner similar to that of the cortical influence on SpV responses (Jacquin *et al.*, 1990). Second, weak SpV inputs to individual barreloids may relay excitatory multiwhisker inputs directly to a barreloid. Third, SpV inputs to extra- and inter-barreloid regions could synapse upon VPM dendrites that span beyond a barreloid's borders. Whether the latter occurs has yet to be tested directly, although it is likely to occur because VPM dendritic trees (Harris, 1986; Chiaia *et al.*, 1991b) certainly sample a greater area than that of a single barreloid. Fourth, VPM multiwhisker sensitivity may simply be due to direct transmission of multiwhisker receptive fields in PrV cells. Jacquin *et al.* (1988) reported, based on hand-held receptive field mapping methods in barbiturate anaesthetized rats, that only 20% of PrV cells are multiwhisker-sensitive. A recent analysis using more carefully controlled, electromechanical whisker deflection and computer-assisted analyses (Doherty *et al.*, 1993) indicates that multiwhisker-sensitive cells constitute 23% of the thalamic projecting PrV cells. Therefore, given the nearly tenfold difference in the sheer numbers of thalamic-projecting cells in PrV and SpV (e.g. Bruce *et al.*, 1987), PrV may represent the major source for multiwhisker convergence in VPM cells.

Acknowledgements

This work was supported by grants DE07662, DE07734, NS29885, NS17763 (M. F. J.) and NS23805 (D. S. Z.) from the National Institutes of Health, United States Public Health Service. We thank Dr Mathew Diamond for a critical reading of the manuscript and Nanci Hobart, Pamela Robinson and Evelyn Williams for expert technical assistance.

Abbreviations

ABC	avidin–biotin–peroxidase complex
CTB	cholera toxin subunit B
HRP	horseradish peroxidase
PO	posterior thalamic nucleus
PrV	principal trigeminal nucleus
SpVc	spinal trigeminal subnucleus caudalis
SpVi	spinal trigeminal subnucleus interpolaris
SpVo	spinal trigeminal subnucleus oralis
TBS–TX	Tris-buffered saline with Triton-X
TMB	tetramethylbenzidine
V	trigeminal
VPL	ventroposterolateral thalamic nucleus
VPM	ventroposteromedial thalamic nucleus
WGA–HRP	wheatgerm agglutinin–horseradish peroxidase

References

Aldes, L. D. and Boone, T. B. (1984) A combined flat-embedding, HRP histochemical method for correlative light and electron microscopic study of single neurons. *J. Neurosci. Res.*, **11**, 27–34.

Armstrong-James, M. and Callahan, C. A. (1991) Thalamo-cortical processing of vibrissal information in the rat. II. Spatiotemporal convergence in the thalamic ventroposterior medial nucleus (VPm) and its relevance to generation of receptive fields of S1 cortical 'barrel' neurons. *J. Comp. Neurol.*, **303**, 211–224.

Armstrong-James, M., Callahan, C. A. and Friedman, M. A. (1991) Thalamo-cortical processing of vibrissal information in the rat. I. Intracortical origins of surround but not centre-receptive fields of layer IV neurones in the rat S1 barrel cortex. *J. Comp. Neurol.*, **303**, 193–210.

Barbaresi, P., Spreafico, R., Frassoni, C. and Rustioni, A. (1986) GABAergic neurons are present in the dorsal column nuclei but not in the ventroposterior complex of rats. *Brain Res.*, **382**, 305–326.

Bates, C. A., Erzurumlu, R. S. and Killackey, H. P. (1982) Central correlates of peripheral alterations in the trigeminal system of the rat. III. Neurons of the principal sensory nucleus. *Dev. Brain Res.*, **5**, 108–113.

Bennett-Clarke, C. A., Chiaia, N. L., Jacquin, M. F. and Rhoades, R. W. (1992) Parvalbumin and calbindin immunocytochemistry reveal functionally distinct cell groups and vibrissa-related patterns in the trigeminal brainstem complex of the adult rat. *J. Comp. Neurol.*, **320**, 323–338.

Brown, A. W. S. and Waite, P. M. E. (1974) Responses in the rat thalamus to whisker movements produced by motor nerve stimulation. *J. Physiol. (Lond.)*, **238**, 387–401.

Bruce, L. L., McHaffie, J. G. and Stein, B. E. (1987) The organization of trigeminotectal and trigeminothalamic neurons in rodents: A double-labeling study with fluorescent dyes. *J. Comp. Neurol.*, **262**, 315–330.

Chiaia, N. L., Rhoades, R. W., Bennett-Clarke, C. A., Fish, S. E. and Killackey, H. P. (1991a) Thalamic processing of vibrissal information in the rat. I. Afferent input to the medial ventral posterior and posterior nuclei. *J. Comp. Neurol.*, **314**, 201–216.

Chiaia, N. L., Rhoades, R. W., Fish, S. E. and Killackey, H. P. (1991b) Thalamic processing of vibrissal information in the rat. II. Morphological and functional properties of medial ventral posterior nucleus and posterior nucleus neurons. *J. Comp. Neurol.*, **314**, 217–236.

Chmielowska, J., Carvell, G. E. and Simons, D. J. (1989) Spatial organization of thalamocortical and corticothalamic projection systems in the rat SmI barrel cortex. *J. Comp. Neurol.*, **285**, 325–338.

De Biasi, S., Frassoni, C. and Spreafico, R. (1988) The intrinsic organization of the ventroposterolateral nucleus and related reticular thalamic nucleus of the rat: A double-labeling ultrastructural investigation with gamma-aminobutyric acid immunogold staining and lectin-conjugated horseradish peroxidase. *Somatosens. Res.*, **5**, 187–203.

Diamond, M. E., Armstrong-James, M., Budway, M. J. and Ebner, F. F. (1992a) Somatic sensory responses in the rostral sector of the posterior group (POm) and in the ventral posterior medial nucleus (VPM) of the rat thalamus: dependence on the barrel field cortex. *J. Comp. Neurol.*, **319**, 66–84.

Diamond, M. E., Armstrong-James, M. and Ebner, F. F. (1992b) Somatic sensory responses in the rostral sector of the posterior group (POm) and in the ventral posterior medial nucleus (VPM) of the rat thalamus. *J. Comp. Neurol.*, **318**, 462–476.

Doherty, D. W., Jacquin, M. F. and Killackey, H. P. (1993) Quantitative analysis of receptive field properties in the rat nucleus principalis. *Soc. Neurosci. Abstr.*, **19**, 327.

Dostrovsky, J. O. and Guilbaud, G. (1988) Noxious stimuli excite neurons in nucleus submedius of the normal and arthritic rat. *Brain Res.*, **460**, 269–280.

Erzurumlu, R. S. and Killackey, H. P. (1980) Diencephalic projections of the subnucleus interpolaris of the brainstem trigeminal complex in the rat. *Neuroscience*, **5**, 1891–1901.

Erzurumlu, R. S., Bates, C. A. and Killackey, H. P. (1980) Differential organization of thalamic projection cells in the brain stem trigeminal complex of the rat. *Brain Res.*, **198**, 427–433.

Harris, R. M. (1986) Morphology of physiologically identified thalamocortical relay neurons in the rat ventrobasal thalamus. *J. Comp. Neurol.*, **251**, 491–505.

Harris, R. M. (1987) Axon collaterals in the thalamic reticular nucleus from thalamocortical neurons of the rat ventrobasal thalamus. *J. Comp. Neurol.*, **258**, 397–406.

Hoogland, P. V., Welker, E. and Van der Loos, H. (1987) Organization of the projections from barrel cortex to thalamus in mice studied with *Phaseolus vulgaris*-leucoagglutinin and HRP. *Exp. Brain Res.*, **68**, 73–87.

Ito, M. (1988) Response properties and topography of vibrissa sensitive VPM neurons in the rat. *J. Neurophysiol.*, **60**, 1181–1197.

Jacquin, M. F. (1989) Structure–function relationships in rat brainstem subnucleus interpolaris. V. Functional consequences of neonatal infraorbital nerve section. *J. Comp. Neurol.*, **282**, 63–79.

Jacquin, M. F. and Rhoades, R. W. (1990) Structure and response properties of cells in trigeminal subnucleus oralis. *Somatosens. Mot. Res.*, **7**, 265–288.

Jacquin, M. F., Mooney, R. D. and Rhoades, R. W. (1986a) Morphology, response properties, and collateral projections of trigeminothalamic neurons in brainstem subnucleus interpolaris of rat. *Exp. Brain Res.*, **61**, 457–468.

Jacquin, M. F., Renehan, W. E., Mooney, R. D. and Rhoades, R. W. (1986b) Structure–function relationships in rat medullary and cervical dorsal horns. I. Trigeminal primary afferents. *J. Neurophysiol.*, **55**, 1153–1186.

Jacquin, M. F., Woerner, D., Szczepanik, A. M., Riecker, V., Mooney, R. D. and Rhoades, R. W. (1986c) Structure–function relationships in rat brainstem subnucleus interpolaris. I. Vibrissa primary afferents. *J. Comp. Neurol.*, **243**, 266–279.

Jacquin, M. F., Golden, J. and Panneton, W. M. (1988) Structure and function of barrel 'precursor' cells in trigeminal nucleus principalis. *Dev. Brain Res.*, **43**, 309–314.

Jacquin, M. F., Barcia, M. and Rhoades, R. W. (1989) Structure–function relationships in rat brainstem subnucleus interpolaris. IV. Projection neurons. *J. Comp. Neurol.*, **282**, 45–62.

Jacquin, M. F., Wiegand, M. and Renehan, W. E. (1990) Structure–function relationships in rat brainstem subnucleus interpolaris. VIII. Cortical inputs. *J. Neurophysiol.*, **64**, 3–27.

Jones, E. G. (1985) *The Thalamus*. Plenum, New York.

Jones, E. G. and Diamond, I. (1994) *Barrel Cortex, Vol. 11. Cerebral Cortex*. Plenum, New York, in press.

Killackey, H. P., Koralek, K.-A., Chiaia, N. L. and Rhoades, R. W. (1989) Laminar and areal differences in the origin of the subcortical projection neurons of the rat somatosensory cortex. *J. Comp. Neurol.*, **282**, 428–445.

Killackey, H. P., Jacquin, M. F. and Rhoades, R. W. (1990) Development of somatosensory system structures. In Coleman, J. R. (ed.), *Development of Sensory Systems in Mammals*. Wiley, New York, pp. 403–429.

Koch, C., Poggio, T. and Torre, V. (1983) Non-linear interactions in a dendritic tree: localization, timing and role in information processing. *Proc. Natl. Acad. Sci. USA*, **80**, 2799–2802.

Land, P. W. and Simons, D. J. (1985) Metabolic and structural correlates of the vibrissae representation in the thalamus of the adult rat. *Neurosci. Lett.*, **60**, 319–324.

Lee, S. M., Friedberg, M. H. and Ebner, F. F. (1993) The role of GABA-mediated inhibition in the rat ventral posterior medial (VPM) thalamus. I: Quantitative assessment of receptive field changes following excitotoxic lesion of the thalamic reticular nucleus. *J. Neurophysiol.*, in press.

Ma, W., Peschanski, M. and Ralston, H. J., III (1986) The overlap of spinothalamic and dorsal column nuclei projection in the ventrobasal complex of the rat thalamus: A double anterograde labeling study using light microscopic analysis. *J. Comp. Neurol.*, **245**, 531–540.

Ma, W., Peschanski, M. and Ralston, H. J., III (1987) The differential synaptic organization of the spinal and lemniscal projections to the ventrobasal complex of the rat thalamus. Evidence for convergence of the two systems upon single thalamic neurons. *Neuroscience*, **22**, 925–934.

Ma, W., Peschanski, M. and Ohara, P. T. (1988) Fine structure of the dorsal part of the nucleus submedius of the rat thalamus: An anatomical study with reference to possible pain pathways. *Neuroscience*, **26**, 147–159.

Mesulam, M.-M. (1982) *Tracing Neural Connections with Horseradish Peroxidase*. Wiley, New York.

Miletic, V. and Coffield, J. A. (1989) Responses of neurons in the rat nucleus submedius to noxious and innocuous mechanical cutaneous stimuli. *Somatosens. Mot. Res.*, **6**, 567–587.

Nicolelis, M. A. L., Chapin, J. K. and Lin, R. C. S. (1992) Somatotopic maps within the zona incerta relay parallel GABAergic somatosensory pathways to the neocortex, superior colliculus, and brainstem. *Brain Res.*, **577**, 134–141.

Ohara, P. T. and Lieberman, A. R. (1985) The thalamic reticular nucleus of the adult rat: experimental anatomical studies. *J. Neurocytol.*, **14**, 365–411.

Peschanski, M. (1984) Trigeminal afferents to the diencephalon in the rat. *Neuroscience*, **12**, 465–487.

Peschanski, M., Lee, C. L. and Ralston, H. J., III (1984) The structural organization of the ventrobasal complex of the rat as revealed by the analysis of physiologically characterized neurons injected intracellularly with horseradish peroxidase. *Brain Res.*, **279**, 63–74.

Peschanski, M., Roudier, F. and Ralston, H. J., III (1985) Ultrastructural analysis of the terminals of various somatosensory pathways in the ventrobasal complex of the rat thalamus: an electron microscopic study using wheatgerm agglutinin conjugated to horseradish peroxidase as an axonal tracer. *Somatosens. Res.*, **3**, 75–87.

Ralston, H. J., III, Ohara, P. T., Ralston, D. D. and Chazal, G. (1988) The neuronal and synaptic organization of the cat and primate somatosensory thalamus. In Bentivoglio, M. and Spreafico, R. (eds), *Cellular Thalamic Mechanisms*. Elsevier, Amsterdam, pp. 127–141.

Rausell, E. and Jones, E. G. (1991a) Histochemical and immunocytochemical compartments of the thalamic VPM nucleus in monkeys and their relationship to the representational map. *J. Neurosci.*, **11**, 210–225.

Rausell, E. and Jones, E. G. (1991b) Chemically distinct compartments of the thalamic VPM nucleus in monkeys relay principal and spinal trigeminal pathways to different layers of the somatosensory cortex. *J. Neurosci.*, **11**, 226–237.

Rausell, E., Bae, C. S., Vinuela, A., Huntley, G. W. and Jones, E. G. (1992) Calbindin and parvalbumin cells in monkey VPL thalamic nucleus: distribution, laminar cortical projections, and relations to spinothalamic terminations. *J. Neurosci.*, **12**, 4088–4111.

Renehan, W. E., Jacquin, M. F., Mooney, R. D. and Rhoades, R. W. (1986) Structure–function relationships in rat medullary and cervical dorsal horns. II. Medullary dorsal horn cells. *J. Neurophysiol.*, **55**, 1187–1201.

Rhoades, R. W., Belford, G. R. and Killackey, H. P. (1987) Receptive field properties of rat VPM neurons before and after selective kainic acid lesions of the trigeminal brainstem complex. *J. Neurophysiol.*, **57**, 1577–1600.

Roger, M. and Cadusseau, J. (1985) Afferents to the zona incerta in the rat: a combined retrograde and anterograde study. *J. Comp. Neurol.*, **241**, 480–492.

Rye, D. B., Saper, C. B. and Wainer, B. H. (1984) Stabilization of the tetramethylbenzidine (TMB) reaction product: application for retrograde and anterograde tracing, and combination with immunohistochemistry. *J. Histochem. Cytochem.*, **32**, 1145–1153.

Schonitzer, K. and Hollander, H. (1981) Anterograde tracing of horseradish peroxidase (HRP) with electron microscope using the tetramethylbenzidine reaction. *J. Neurosci. Methods*, **4**, 373–383.

Shammah-Lagnado, S. J., Negrao, N. and Ricardo, J. A. (1985) Afferent connections of the zona incerta: a horseradish peroxidase study in the rat. *Neuroscience*, **15**, 109–134.

Simons, D. J. and Carvell, G. E. (1989) Thalamocortical response transformation in the rat vibrissa/barrel system. *J. Neurophysiol.*, **61**, 311–330.

Stone, J. (1983) *Parallel Processing in the Visual System: The Classification of Retinal Ganglion Cells and Its Impact on the Neurobiology of Vision*. Plenum, New York.

Sugitani, M., Yano, J., Sugai, T. and Ooyama, H. (1988) Separation of the ventrobasal complex into VPM and VPL in the rat: a mapping study based on receptive fields of single neurons. *J. Kanazawa Med. Univ.*, **13**, 322–327.

Van der Loos, H. (1976) Barreloids in mouse somatosensory thalamus. *Neurosci. Lett.*, **2**, 1–6.

Waite, P. M. E. (1973) The responses of cells in the rat thalamus to mechanical movements of the whiskers. *J. Physiol. (Lond.)*, **228**, 541–561.

Welker, E., Hoogland, P. V. and Van der Loos, H. (1988) Organization of feedback and feedforward projections of the barrel cortex: a PHA-L study in the mouse. *Exp. Brain Res.*, **73**, 411–435.

White, E. (1989) *Cortical Circuits: Synaptic Organization of the Cerebral Cortex—Structure, Function and Theory*. Birkhauser, Boston.

Williams, M. N., Zahm, D. S. and Jacquin, M. F. (1993) Parvalbumin, calbindin and trigeminal immunostaining patterns in rat thalamus. *Soc. Neurosci. Abstr.*, **19**, 515.

Woolsey, T. A. (1990) Peripheral alteration and somatosensory development. In Coleman, J. R. (ed.), *Development of Sensory Systems in Mammals*. Wiley, New York, pp. 461–516.

Woolston, D. C., La Londe, J. R. and Gibson, J. M. (1982) Comparison of the response properties of cerebellar- and thalamic-projecting interpolaris neurons. *J. Neurophysiol.*, **48**, 160–173.

Yoshida, A., Dostrovsky, J. O., Sessle, B. J. and Chiang, C. Y. (1991) Trigeminal projections to the nucleus submedius of the thalamus in the rat. *J. Comp. Neurol.*, **307**, 609–625.